

Modifications to Foam Volume Measurements

Ryan Cunningham

Department of Mining and Materials Engineering

McGill University

Montreal, Canada

December 2009

A thesis submitted to the office of graduate studies and research in partial fulfilment
of the requirements for the degree of masters of engineering

© Ryan Cunningham (2009)

ABSTRACT

The amount of foam volume generated in relation to the gas flowrate has long been used to define the foaminess of a solution and to characterize surfactants. The vessel geometry and gas flowrate range can affect the foam volume results. A fixed area column was tested alongside a variable area conical vessel with three surfactants (commercial frothers). It was found that the fixed area vessel would cause foam volume to expand or contract, which masks the effect of the surfactant. The conical vessel showed two regimes of foam volume production dependant on gas flowrate. The low gas flowrate regime was tentatively associated with a quiescent bubbly zone while the high gas flowrate regime associated to a turbulent bubbly zone. Foaming properties of a surfactant are best determined with a variable area vessel at low gas flowrate.

RÉSUMÉ

L'étude du volume de mousse généré en corrélation avec le flux de gaz est utilisée depuis longtemps afin de déterminer la moussabilité d'une solution et d'en caractériser les agents de surface. La géométrie de la cuve ainsi que l'amplitude du flux de gaz sont connus pour avoir un effet sur les résultats de volume de mousse généré. Une colonne avec une aire de surface prédéfinie a été testée en parallèle avec une cuve conique de surface variable ; trois agents de surface (des moussants commerciaux) ont servi de base d'étude. Les résultats ont montré que la cuve possédant une aire de surface fixe causerait l'expansion ou la contraction de la mousse, masquant l'effet de l'agent de surface. Avec la cuve conique, deux régimes de production du volume de mousse, chacun dépendants du flux de gaz, ont été déterminés. Le régime correspondant à un flux de gaz faible est le produit d'une zone quiescente d'évolution des bulles alors que le régime correspondant à un flux de gaz élevé montre des propriétés typiquement cinématiques dues à une zone turbulente d'évolution des bulles. Les propriétés de moussage d'un agent de surface donné sont déterminées avec une meilleure exactitude en utilisant une cuve de surface variable avec un flux de gaz faible.

ACKNOWLEDGEMENTS

To my supervisor, Professor James A. Finch, I would like to thank for being a teacher. He has taught me the benefits of seeing the best in everybody around him; being continuously open to new ideas; and providing proof that energy can be seemingly boundless in a human. Our discussions have been a source of delight throughout the years. It was he who introduced me to the world of research and, more importantly, the world of bubbles.

I would like to acknowledge the mineral processing group for all their help and constructive suggestions and comments. I extend a special thanks to Ray, Monique, Dr.Rao and Barbara for their help and encouragement.

I thank all the friends I've met along the way for the laughs, the memories and the occasional pint.

I would like to acknowledge my parents for teaching me how to be a focused worker and to always challenge myself. All my successes are, in part, due to their guiding influence and love throughout my life. When I feel like I am low on strength, my family has always been there to give theirs.

I want to thank my wife for sharing the adventure with me. I travelled half the globe to find her and I hope to travel the other half with her. I thank her for the continuous love, encouragement and motivation she gives me.

TABLE OF CONTENTS

ABSTRACT	2
RÉSUMÉ	3
ACKNOWLEDGMENTS	4
TABLE OF CONTENTS	5
LIST OF FIGURES	7
LIST OF TABLES	9
NOTE TO READER	10
CHAPTER 1:	11
FOAM STRUCTURE IN DYNAMIC FOAM TESTS WITH A FIXED AREA VESSEL	11
INTRODUCTION	11
STRUCTURE OF FOAM: BACKGROUND THEORY	12
THE FORCES AT PLAY	15
DYNAMIC TEST: BACKGROUND THEORY	20
EXPERIMENTAL	23
FOAMING VESSEL	23
SURFACTANTS	24
FOAM VOLUME	24
FOAM STRUCTURE	24
LIQUID FRACTION OF FOAM AND BUBBLING REGION	24
RESULTS	25
FOAM VOLUME	25
FOAM STRUCTURE	27
LIQUID FRACTION OF FOAM AND BUBBLY REGION	30
DISCUSSION	33
CONCLUSIONS	34
REFERENCES	34

CHAPTER 2:	37
FOAM VOLUME MEASUREMENTS WITH A VARIABLE AREA VESSEL	37
INTRODUCTION	37
WATKINS FUNNEL: BACKGROUND THEORY	37
PYSIOCHEMICAL/KINEMATIC REGIMES: BACKGROUND THEORY	38
EXPERIMENTAL	40
FOAMING VESSEL	40
FOAM VOLUME MEASUREMENT	42
SURFACTANTS	42
RESULTS	43
HYSTERESIS	43
LOW/HIGH GAS FLOWRATE REGIME TRANSITION	44
FOAM STABILITY	45
TRANSITION GAS FLOWRATE	47
FOAM STABILITY AT HIGH/LOW GAS FLOWRATES	48
CONCLUSIONS	51
REFERENCES	51
CHAPTER 3:	53
COMPARISON OF A CONICAL VERSUS A CYLINDRICAL FOAMING VESSEL	54
INTRODUCTION	54
THEORY	55
EXPERIMENTAL	56
FOAMING VESSEL	56
FOAM VOLUME MEASUREMENT	57
SURFACTANTS	58
RESULTS	59
FOAMABILITY	59
TRANSITION GAS FLOWRATE ANALYSIS	63
FOAMABILITY	65
CONCLUSION	69
REFERENCES	69

LIST OF FIGURES

CHAPTER 1: **11**

FIGURE 1: REGIONS OF A FOAM SEEN IN AN OVERFLOWING FOAM COLUMN WITH WASH WATER INJECTION (AFTER(YIANATOS ET AL., 1986)).13

FIGURE 2: STRUCTURE OF CLASSICAL POLYHEDRAL FOAM. A) FOAM FILM BETWEEN TWO AIR BUBBLES; B) PLATEAU BORDER WHERE THREE FILMS MEET.15

FIGURE 3: THE FIVE STAGES OF FILM THINNING. THE FIRST STAGE IS “NO INTERACTION” AND THE LAST STAGE IS “RUPTURE”..18

FIGURE 4: TERMS INTRODUCED FOR SYSTEM AT REST AND A BUBBLING SYSTEM.22

FIGURE 5: THE EFFECT OF SUPERFICIAL GAS VELOCITY (CM/S), J_G , ON FOAM HEIGHT (CM).26

FIGURE 6: IMAGES OF FOAM FORMED WITH 10 PPM F150 AT DIFFERENT SUPERFICIAL GAS VELOCITIES.....28

FIGURE 7: IMAGE OF FOAM FORMED WITH 10 PPM F150 AT DIFFERENT SUPERFICIAL GAS VELOCITIES.....29

FIGURE 8: HYDROSTATIC PRESSURE PROFILES USED TO CALCULATE GAS HOLDUP OF BUBBLY ZONE AND FOAM ZONE OF SYSTEMS AT DIFFERENT SUPERFICIAL GAS VELOCITY, J_G31

FIGURE 9: GAS HOLDUP IN BUBBLY AND FOAM ZONES.32

FIGURE 10: THE REGIONS OF FOAM STABILITY DUE TO THE FIXED AREA VESSEL’S GEOMETRY..33

CHAPTER 2: **37**

FIGURE 1: CONICAL FOAM TEST APPARATUS SCHEMATIC WITH NOMENCLATURE.....41

FIGURE 2: HYSTERESIS LOOP OF THE CONICAL VESSEL.43

FIGURE 3: EXAMPLE OF EQUATION 6 BEING FIT TO BOTH A 1PPM F150 AND 10PPM F150 DATA SET.....	46
FIGURE 4: TRANSITION GAS FLOWRATE VALUES.....	47
FIGURE 5: FOAM STABILITY (S) FOR RANGES OF GAS FLOWRATES BELOW AND ABOVE THE TRANSITION GAS FLOWRATE VALUE.	49
FIGURE 6: FROTHER CONCENTRATION EFFECT ON THE GIBBS-MARANGONI FILM ELASTICITY.	50
CHAPTER 3:	53
FIGURE 1: FOAMABILITY BEHAVIOR IN A FIXED AREA VESSEL AND A VARIABLE AREA VESSEL.	55
FIGURE 2: CYLINDRICAL AND CONICAL FOAMING VESSELS.	56
FIGURE 3: 3-FACTOR, 2-LEVEL DESIGN USED TO TEST WHICH PARAMETERS AFFECT FOAMABILITY.	58
FIGURE 4: 3-FACTOR, 2-LEVEL DESIGN USED TO TEST WHICH PARAMETERS AFFECT THE GAS TRANSITION VALUE.	58
FIGURE 5: FOAMABILITY OF 3 PPM F150.....	60
FIGURE 6: FOAMABILITY OF 30 PPM F150.....	60
FIGURE 7: FOAMABILITY OF 10 PPM MIBC.....	61
FIGURE 8: FOAMABILITY OF 100 PPM MIBC.....	61
FIGURE 9: TRANSITION GAS FLOWRATE VALUE, PRIMARY AND SECONDARY INTERACTIONS.....	63
FIGURE 10: PRIMARY INTERACTION FOR FOAMABILITY OF MIBC AND F150.....	65
FIGURE 11: SECONDARY INTERACTION FOR FOAMABILITY OF MIBC AND F150.....	66
FIGURE 12: ILLUSTRATION OF HOW A STRONG GIBBS-MARANGONI EFFECT MAY INITIATE FILM RUPTURE BY CREATING LOCAL TENSION.	67

LIST OF TABLES

CHAPTER 1:	11
TABLE 1– FROTHER USED IN FOAM VOLUME EXPERIMENTS.....	24
TABLE 2 – STABILITY OF FOAM AT DIFFERENT CONCENTRATIONS AND AT DIFFERENT J_G (STABILITY) REGIMES.....	27
CHAPTER 2:	37
TABLE 1- FROTHERS USED IN FOAM VOLUME EXPERIMENTS.....	42
TABLE 2 -TRANSITION GAS FLOWRATE VALUES (χ_0) AND THE FOAM STABILITY FOR REGION BELOW THE TRANSITION ($\alpha_1 - \alpha_2$) AND ABOVE ($\alpha_1 + \alpha_2$).....	46
CHAPTER 3:	53
TABLE 1– FROTHERS USED IN FOAM VOLUME EXPERIMENTS.....	57
TABLE 2- COMPARISON OF FOAMABILITY FOR THE UPPER GAS FLOWRATE REGIME OF THE CONICAL VESSEL TO THE LOWER GAS FLOWRATE REGIME OF THE CYLINDRICAL VESSEL.....	59
TABLE 3- COEFFICIENTS OF INTERACTION FOR TRANSITION GAS FLOWRATE VALUES	62
TABLE 4- COEFFICIENTS OF INTERACTION FOR F150	64
TABLE 5- COEFFICIENTS OF INTERACTION FOR MIBC.....	64

NOTE TO READER

The following thesis is organized into three chapters:

- Chapter 1 investigates the traditional method of foam volume measurements, a fixed area cylindrical column, as an appropriate vessel for the study of flotation frothers.
- Chapter 2 examines a variable area conical vessel as a foam volume measurement device for frother studies in lieu of a fixed area vessel.
- Chapter 3 directly compares the two vessel types.

Please note that each chapter has its own introduction and conclusions.

CHAPTER 1:

FOAM STRUCTURE IN DYNAMIC FOAM TESTS WITH A FIXED AREA VESSEL

INTRODUCTION

The need to measure and understand froth in flotation systems requires little explanation: it influences overall recovery and selectivity. With this appreciated, one difficulty lies in how to quantify froth properties. There is still no agreement on a parameter that characterizes foaminess (Bikerman, 1973).

The flotation literature uses both the term froth and foam. The distinction is that foam refers to two-phase systems (i.e., no solids) and froth to three-phase systems. The distinction will be used here. Foams formed by the surfactants used in flotation (frothers) are described as “wet”. Frothers are non-ionic surfactants providing relatively unstable foams compared to ionic surfactants (Wang and Yoon, 2008b) and the concentrations used are relatively low (well below the critical micelle concentration (cmc)). Liquid content in foams formed with frothers has been measured up to 40 vol% (Malysa et al., 1981) whereas the majority of foam research and models do not consider foams with a liquid content greater than 10 vol% (Safouane et al., 2006, Koehler et al., 2000, Cox et al., 2000).

Foams formed by frothers are thus classed as unstable or transient. As a distinction, the lifetime of a single bubble rising to the surface of a foam created with frother would be measured in seconds, whereas the majority of surfactants used in foam research would see a bubble life time measured in minutes, or even hours. The explanation is that

flotation systems do not want persistent froths as they cause downstream problems in equipment such as pumps.

Regardless of what is measured, traditional foam experiments use a fixed cross-sectional area vessel, typically a column. We will question this traditional technique looking to uncover the biases associated with a fixed area vessel. The theoretical explanations employed for “classical” foam stability will be reviewed for foams formed with “non-classical” frother surfactants.

STRUCTURE OF FOAM: BACKGROUND THEORY

The classical structure of foams considers highly polygonal cellular air bubbles separated by thin films of the surfactant solution. Foams formed with frothers can reach this structure but not before evolving through a series of prior stages where the bubbles remain largely spherical. The different structures have been documented using an overflowing foam column with water injection into the foam (referred to as ‘wash water’) used to preserve frother foams to measurable heights (Yianatos et al., 1986). This structure means different liquid fractions exist along the vertical profile. Foam structure can be associated with a range of liquid fractions (Figure 1). The amount of liquid relative to gas will mark the difference between spherical bubbles and polygonal cellular bubbles.

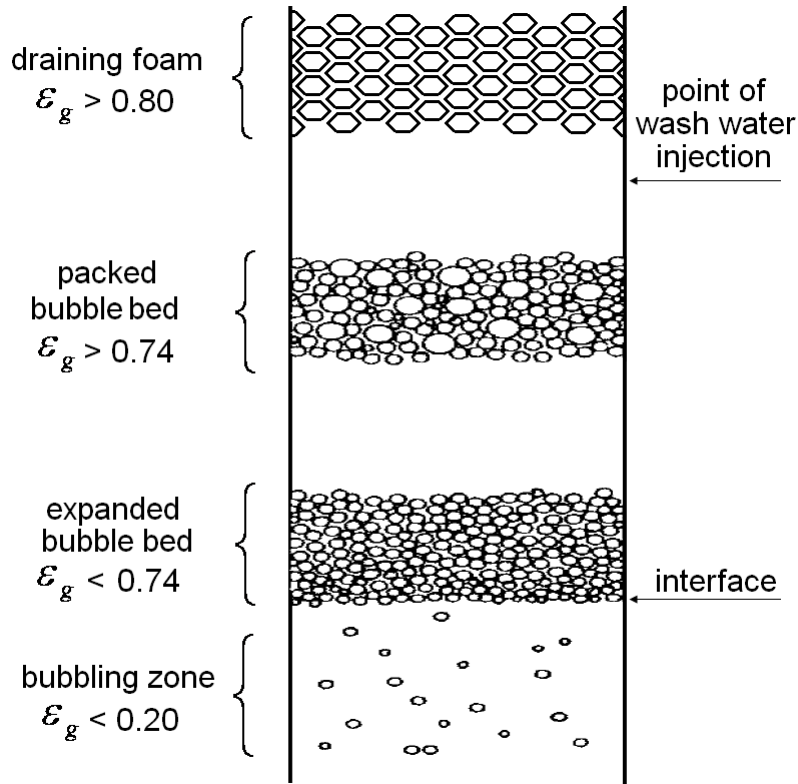


Figure 1: Regions of a foam seen in an overflowing foam column with wash water injection (after(Yianatos et al., 1986)).

Bubbles are generated in aqueous frother solution in the region known as the bubbling zone (in two-phase) and pulp zone (in three-phase). This zone has a gas volume fraction (gas holdup) less than 20 vol%. The bubbling zone is separated from the foam by a visible and definite interface. Bubbles decrease their velocity by 4 to 5 fold at the interface and the volume fraction of gas increases up to 74 vol% (Yianatos et al., 1986). The region in which the increase of volume fraction takes place is known as the expanded bubble bed. The expanded bubble bed or *kugelschaum* (sphere foam) consists of spherical bubbles separated by thick films of viscous liquid (Pugh, 1996). This region usually escapes attention as it takes place quickly over the span of a two or three bubble diameters. In the case with significant wash water injection this region can be observed and indentified (Yianatos et al., 1986). The nature of the expanded bubble bed, with

water being squeezed from between the bubbles arranging themselves into a foam structure, has been likened to an inverse fluidized bed (Haas and Johnson, 2002). This analogy is important as the drainage of classical foam is seen as taking place in narrow channels between tightly packed bubbles dominated by physiochemical forces such as capillary and dispersion forces (Safouane et al., 2006, Koehler et al., 2000, Cox et al., 2000, Neethling et al., 2002). In the case of the expanded bubble bed, the forces are hydrodynamic in nature. The liquid drainage can be analysed as passage through many parallel pipes of various cross section (Yianatos et al., 1986).

When gas fraction rises above 74 vol%, sufficient water has been squeezed out from between bubbles to initiate point contacts (Kann and Feklistov, 1977). This is the juncture when bubbles no longer maintain their spherical shape. Films begin to form (Figure 2a) between bubbles and Plateau borders (Figure 2b) form where films meet. The region where gas bubble structure changes from spherical to polygonal is the packed bubble bed. It is here that the governing forces shift from hydrodynamic to physiochemical. In the case of a column with wash water, it is only above the point of wash water injection that classical foam structure is evident at a gas fraction above 80 vol% (Yianatos et al., 1986) and is referred to as the draining foam region. Bubbles are polyhedral gas cells with flat walls and separated by thin films. The polyhedra are almost regular dodecahedra (Pugh, 1996). It will be in this region that physiochemical forces dominate stability and drainage of water.

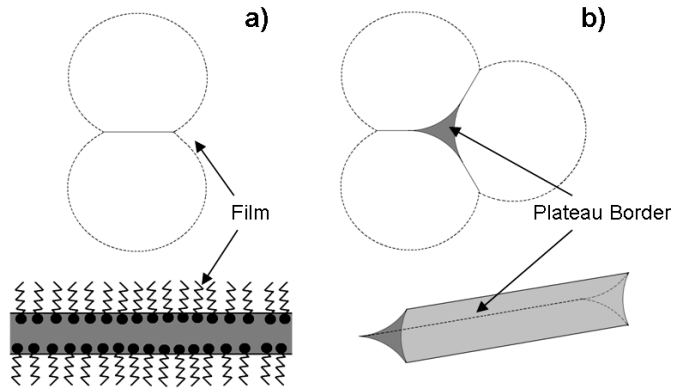


Figure 2: Structure of classical polyhedral foam. a) Foam film between two air bubbles; b) Plateau border where three films meet.

THE FORCES AT PLAY

All foams are thermodynamically unstable. The interface between gas and solution represents a significant fraction of the system's free energy. Considering that the foam will collapse, it would be inaccurate to look for a force balance within the foam. It is better to divide the forces into two categories: the forces that drive solution drainage (and ultimately foam collapse); and the forces that resist solution drainage (Ivanov, 1980, Pugh, 1996).

Water drainage occurs in films and Plateau borders. Films form when sufficient water has drained between two adjacent bubble surfaces. Plateau borders form at the intersection of three films. In drainage models, different mechanisms of drainage are assigned to Plateau borders and to films (Pugh, 1996). The forces that can manifest in films, are also active in Plateau borders. An important difference is that over the life time of a foam, the net flowrate of solution is from the films to the Plateau borders. As a simplification, Plateau borders can be seen as thick films. The prevalent film forces are a function of film thickness. As a film narrows, the forces shift from hydrodynamic to molecular.

Ivanov (1980) identified five stages of film thinning from two non interacting bubbles (in the bubbly region) to rupture of the film. Figure 3 lists the five stages along with the approximate film thickness at the end of each stage and the forces present at each stage. The film thickness that distinguishes the stages is dependent on bubble size, surface tension and the surfactant. A bubble diameter of 1.5 mm with a solution surface tension of 66 mN/m was selected for the thickness calculations (Ivanov, 1980). The final rupture thickness of 50 nm was selected from a thin film study that used flotation frothers (Wang and Yoon, 2008a).

Bubbles more than 15 mm (surface to surface) apart have no direct interaction. This would describe bubbles in the bubbly region. Two bubble surfaces closer than 15 mm have noticeable interactions leading to surface distortion. This is the commencement of the hydrodynamic interaction stage. Liquid between two surfaces will drain due to gravity (or if one prefers, buoyancy drives the gas to rise above the surrounding liquid). As the solution flows downward through the bed of bubbles the bulk viscosity of the solution controls the drainage rate.

Transformation of the foam into the film and Plateau border structure commences at film thickness less than 350 μm . Surface deformations are a characteristic of this interaction stage. They result from the bubble surface not extending (as bubble moves from spherical to polyhedral) at a uniform rate which creates pressure differences between bubbles resulting in surface deformation. This region

represents a high pressure region in the newly forming film. To stabilize, fluid flows from the film to the Plateau border, a relatively low pressure area. This pressure difference is better known as the capillary pressure. The deformation has a radius of curvature, r , and the capillary pressure is calculated as $\Delta P = (2\gamma)/r$, where γ is the surface tension of the solution. Capillary pressure is a drainage force as it “sucks” liquid from a film. The restorative force, due to non-uniform surface expansion, is the Gibbs-Marangoni effect (Pugh, 1996). As a bubble surface expands at a higher rate in the film than in the Plateau border a lower concentration of frother molecules arises on the bubble surface in the former. Frother molecules lower surface tension through disrupting the H-bonding between water molecules. Therefore when there is a region of low frother concentration and a region of higher frother concentration there is a surface tension gradient increasing towards the low concentration region. The force associated with the gradient resists film thinning (Gibbs elasticity). The force also causes accompanying flow in the adjoining liquid which further resists drainage (Marangoni effect). This is equivalent to frother molecules moving from the high concentration region to the low concentration region. Since frother molecules have a hydrophilic group (usually OH) in their molecular structure which H-bonds with water (Gélinas et al., 2005) this movement of frother can be considered to transport water along with it, again countering drainage. The H-bonded water, due to viscous forces, brings an appreciable amount of “free” water and restores thinning films.

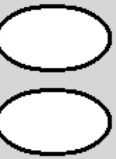
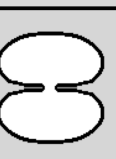
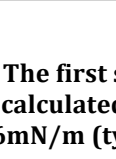
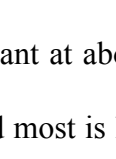
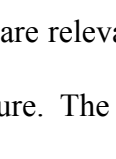
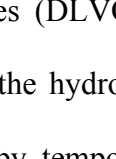
STAGE NAME	FILM THICKNESS		DRAINAGE FORCES	RESISTIVE FORCES
NO INTERACTION	∞			
	$1.5 \times 10^{-2} \text{ m}$			
HYDRODYNAMIC INTERACTION	15 mm		<ul style="list-style-type: none"> • Gravity (<i>Buoyancy</i>) 	<ul style="list-style-type: none"> • Bulk viscosity
	$3.5 \times 10^{-4} \text{ m}$			
INTERFACE INTERACTION	$350 \text{ }\mu\text{m}$		<ul style="list-style-type: none"> • Gravity • Capillary 	<ul style="list-style-type: none"> • Bulk viscosity • Gibbs - Marangoni
	$1.0 \times 10^{-7} \text{ m}$			
THIN FILM INTERACTION	100 nm		<ul style="list-style-type: none"> • Gravity • Capillary 	<ul style="list-style-type: none"> • Gibbs - Marangoni
	$5.0 \times 10^{-8} \text{ m}$		<ul style="list-style-type: none"> • Hydrophobic • Van der Waals 	<ul style="list-style-type: none"> • Surface viscosity
RUPTURE	50 nm			

Figure 3: The five stages of film thinning. The first stage is “no interaction” and the last stage is “rupture”. Film thickness values were calculated with bubbles of 1.5 mm diameters and a solution surface tension of 66mN/m (typical of 10 ppm F150 solution).

Thin film interactions become significant at about 100 nm or less; i.e., when practically all water has drained from the film and most is located in the Plateau borders. It is at this scale that long range molecular forces are relevant to film stability. These film forces are better known as the disjoining pressure. The disjoining pressure is accounted in the electrostatic and van der Waals forces (DLVO theory (Derjaguin and Landau, 1941, Overbeek, 1941, Verwey, 1947) and the hydrophobic force (Wang and Yoon, 2008b). The van der Waals force is caused by temporary dipoles that occur in molecules, a tendency which increases with molecule size. Therefore, the surfactant molecules from

one interface are drawn to the surfactant molecules of the other interface. The hydrophobic force is driven by the lower energy state that would be achieved by the combining of the non-polar gas molecules in separated bubbles. Wang and Yoon (2008a) reported, in a study with flotation frothers, that the van der Waals force was 15-90 times less than the hydrophobic force. While the hydrophobic and the van der Waals forces increase drainage, the electrostatic force slows drainage. The electrostatic force is not included in Figure 3 because frothers are non-ionic. The force is related to the bubble's electric double layer associated with ionic surfactants creating a repulsive force retarding coalescence (i.e., retarding film drainage).

The surface viscosity listed in Figure 3, a resistive force, is in lieu of bulk viscosity. There is debate whether there is a difference between bulk viscosity and the surface viscosity. A higher surface viscosity compared to bulk could be due to the polar OH head group of the frothers forming H-bonds with water and providing some additional structure which resists shear. This viscosity is only appreciable at the nanometre scale.

The rupture of a film is the last stage. Although Figure 3 reports the critical rupture thickness to be ca. 50 nm, film thickness with frothers would likely not reach this value. Film thickness at the nanometre scale is only achievable in a system without turbulence or disturbances. A foam, in reality, is not an assembly of stationary films but a network of inter-connected flow channels. The release of water when bubbles coalesce causes the pressure at the Plateau borders to flux rapidly upon passage of the "freed" film water.

Adding the fact that every bubble colliding with the foam interface passes along its kinetic energy upward into the foam, a foam can be appreciated as a “turbulent” structure.

In a study that compared the stability of a thin film with the stability of a froth column (Malysa et al., 1981), a parameter was found that had an effect on the stability of a single isolated film but had no effect on the stability of the foam column. The explanation was that the parameter had an effect on the thin film forces but the films never reached this thickness in the foam. Foams with flotation frothers fall into the hydrodynamic and interface interactions region and rarely reach the thin film interactions region.

DYNAMIC TEST: BACKGROUND THEORY

There are two families of foam stability test: static and dynamic. The dynamic tests employ a continuous flow of gas and are defined when the system has reached steady state and the maximum (or equilibrium) foam height has been achieved. In other words, the volume of air lost in foam (bubble) breakage at the top is equal to the volume of the air entering the foam as bubbles from the bottom. The measurement of interest in a dynamic test is the equilibrium foam height (or volume depending on geometry). In contrast, a static test involves shutting off the gas and monitoring the foam over a period of time as it collapses. Decay properties, such as foam half-life, are measured.

A dynamic foam test is considered closer to flotation conditions (Barbian et al., 2003). The similarities are the following: air is continuously introduced, an interface forms and bubbles move upward through the foam/froth, with liquid draining downwards meaning

there is a difference in the foam/froth characteristics from top to bottom. The principal difference is that in a dynamic test foam reaches equilibrium height while in flotation froth has a set height.

A dynamic test is also more practical considering the “weak” foaming properties of frothers. A constraint in frother studies is that films have lifetimes usually too short to readily observe. One researcher noted that the films being studied would often rupture before the microscope being used could be focused and proceeded to say that all measurements thus taken should be considered as qualitative (Malysa et al., 1981). Dynamic tests provide foam that can be measured repeatedly and quantitatively.

For the dynamic test two metrics have been proposed: the dynamic foamability index (*DFI*) (Czarnecki et al., 1982) and the unit of foaminess (Σ) (Bikerman, 1938).

The unit of foaminess is represented by Σ with units of time. It is defined as (see also Figure 1):

$$\Sigma = \frac{V_f}{Q} = \frac{h_f A_c}{Q} \quad (1)$$

where V_f is foam volume (m^3), Q is the volumetric flowrate of gas (m^3/s), h_f is the equilibrium foam height (m) and A_c is the cross sectional area of the test vessel (m^2). The Bikerman value represents the lifetime of a bubble from the bottom to the top of the foam. Higher Σ values represent increased bubble lifetimes, equated with increased foam stability.

The dynamic foamability index (*DFI*) was proposed in efforts to define a surfactant by its ability to create foam (Czarnecki et al., 1982). The foam volume (V_f) is measured as a function of gas flowrate and surfactant concentration. The first step in data processing is to plot foam volume (V_f) versus gas flowrate (Q) for a given surfactant concentration, and the retention time (rt) is derived by taking the slope of the foam V_f-Q relationship,

$$rt = \frac{\partial V_f}{\partial Q} \quad (2)$$

Recalling equation 1, retention time (rt) is the same as the Bikerman value (Σ). The second step is to plot rt (or Σ) versus surfactant concentration (c). The *DFI* is determined as follows:

$$DFI = \left(\frac{\partial(\Sigma)}{\partial c} \right)_{c=0} \quad (3)$$

i.e., the *DFI* is the slope of the Bikerman value versus concentration curve as the concentration approaches zero. The claimed advantage of the *DFI* is that it is constant for a given surfactant (Czarnecki et al., 1982).

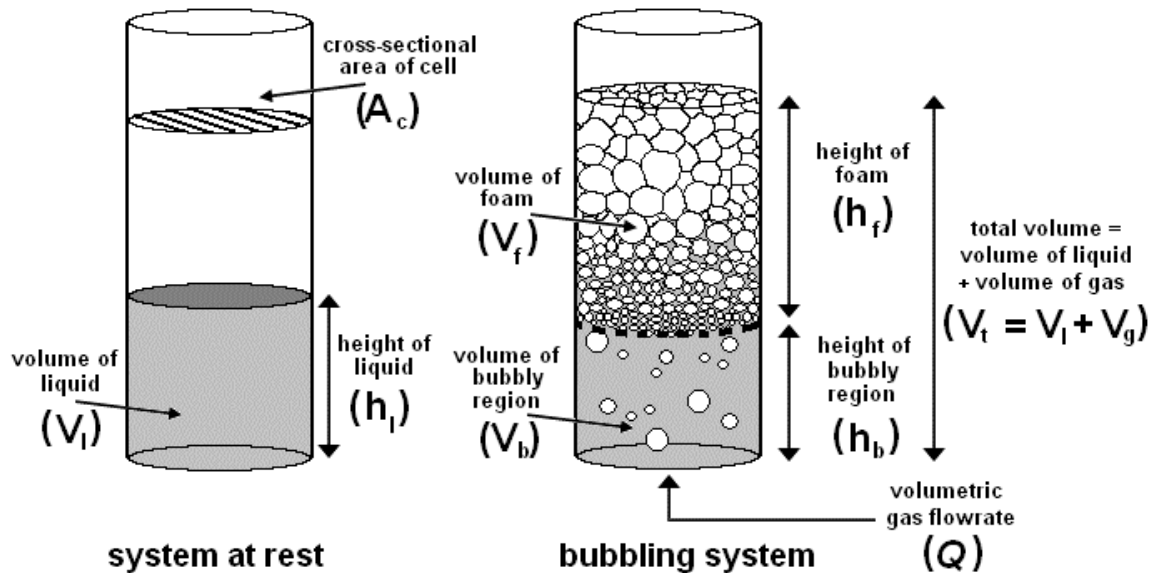


Figure 4: Terms introduced for system at rest and a bubbling system.

The foam volume used by Bikerman (and in determination of *DFI*) (Figure 1) is the difference between the total volume of the foaming column ($V_f + V_b$) and the volume of the liquid (V_l) for the system at rest,

$$V_{foam(original)} = V_t - V_l = V_f + V_b - V_l = V_g \quad (4)$$

i.e., the volume of foam includes the volume of gas (V_g) in both the foam and bubbly regions. This volume of gas can be represented as:

$$V_g = \varepsilon_{g(foam)} V_f + \varepsilon_{g(bubbly\ region)} V_b \quad (5)$$

where $\varepsilon_{g(foam)}$ and $\varepsilon_{g(bubbly\ region)}$ are the gas hold-up (volumetric fraction of air) in the foam and the bubbly region, respectively. V_g is an approximate measurement of V_f as long as $(\varepsilon_{g(foam)} V_f)$ is much greater than $(\varepsilon_{g(bubbly\ region)} V_b)$ and $\varepsilon_{g(foam)} \approx 1$. This condition is approached with some strong foaming surfactants but is not generally true for frothers where V_f is small (usually $< V_b$ depending on experimental set-up), $\varepsilon_{g(bubbly\ region)}$ (fractional) can range from 0.05 to 0.45 (Xu et al., 1991) and $\varepsilon_{g(foam)}$ can be as low as 0.6 (Yianatos et al., 1986). A measurement of foam volume that is independent of the bubbly region requires measuring the volume between the bubbly region/foam interface and the top of the foam.

EXPERIMENTAL

Foaming Vessel

The foaming vessel used was a rectangular column made of Plexiglas with internal dimensions 1 cm x 27.5 cm and height 200 cm. Air bubbles were produced with a coarse frit (nominal pore size 40 - 60 mm) metallic sparger (surface area 28.5 cm²).

Distance from sparger to foam interface was 100 cm for all tests (± 2 cm). The sparger was rinsed in acetone before every test.

Surfactants

The frother used was a commercial flotation frother F150 (see Table 1).

Table 1- Frother used in foam volume experiments

Frother Type	Description	Molecular Weight (g/mol)	Chemical Formula
F150	Polypropylene glycol	425	H-(C ₃ H ₆ O) ₇ -OH

Foam Volume

Foam height was measured visually and used to calculate foam volume ($V_f = h_f A_c$).

There was a two-minute interval between gas flowrate settings.

Foam Structure

Images were taken with the foam at equilibrium using a TroubleShooter HR. Halogen lights with diffuser paper were placed on the opposite side of the foam column to create a high contrast image.

Liquid Fraction of Foam and Bubbling Region

The liquid fraction was measured by a technique attributed to Cutting et al. (1981) that was further refined by Ireland and Jameson (2007). A hydrostatic pressure profile (pressure vs. height) was obtained throughout the bubbling zone and foam. Air was passed through a copper tube to exit (as a bubble) at a measured height in

the column. The pressure was measured with a differential pressure transducer. The gas fraction was calculated by taking the differential of pressure in relation to height (dP/dy) in the following equation:

$$\varepsilon_g = 1 - \left(-\frac{1}{\rho_{liquid} g} \frac{dP}{dy} \right) \quad (6)$$

where ρ_{liquid} is the density of the liquid and g is the gravitational constant.

RESULTS

Foam Volume

The foam volume showed a strong dependence on gas flowrate. Figure 4 shows foam height (h_f , cm) as a function of superficial gas velocity (J_g , derived by dividing the gas flowrate, Q , by the cross sectional area of the column, A , with units in cm/s) for three concentrations of F150. Shown are two distinct $h_f - J_g$ regions corresponding to low and high superficial gas velocity. The low J_g region forms little foam and rate of change in height with gas velocity is small. The change of regime takes place in the J_g range 1.75 cm/s to 2.25 cm/s. At high J_g , foam height is more sensitive to J_g . From J_g of 0 to 2 cm/s, foam height does not exceed 10 cm; from J_g 2 to 4 cm/s foam height reaches the top of the vessel (100 cm). These two regions can be seen in the results from various authors. (Gupta et al., 2007, Laskowski et al., 2003, Czarnecki et al., 1982).

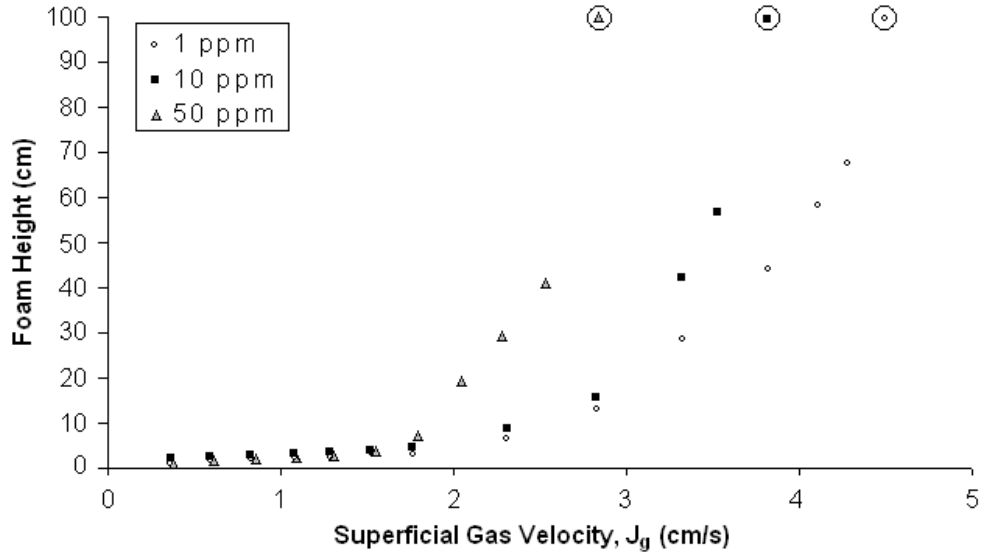


Figure 5: The effect of superficial gas velocity (cm/s), J_g , on foam height (cm). \circ , \blacksquare , \blacktriangle , represent 1, 10, 50 ppm respectively whereas \odot , \blacksquare , \blacktriangle , represent the J_g values at which the 1, 10, 50 ppm systems flooded and filled the 100 cm of the column respectively.

The effect of concentration is not readily discernable in the low J_g region. If foam stability (Σ) is measured from 0 to 1.75 cm/s we observe (Table 2) that Σ decreases with increasing frother concentration. This is contrary to expectation; an increase in concentration is expected to increase foam stability. This suggests that the low J_g region is not dominated by physiochemical forces but rather by hydrodynamics.

The relationship of stability to concentration in the high J_g regime seen in Table 2 is in line with expectation, increased F150 concentration results in greater Σ (i.e., higher foam stability). (Σ was derived by fitting a linear trend through the data above J_g 2.25 cm/s up to the J_g which resulted in flooding (a foam height > 100 cm).

A concentration effect seen in Figure 4 is the J_g value at which the regime change occurs: at 50 ppm the change is around J_g 1.75 cm/s while for 1 ppm the change is at ca. J_g 2.25 cm/s.

Table 2 – Stability of foam at different concentrations and at different J_g (stability) regimes.

Concentration	Stability Regime	Stability (Σ)	Quality of Fit (R^2)
1 ppm	Low	0.96 s	0.97
1 ppm	High	44.88 s	0.89
10 ppm	Low	0.83 s	0.92
10 ppm	High	56.50 s	0.85
50 ppm	Low	0.78 s	0.94
50 ppm	High	75.83 s	0.97

Foam Structure

Images were taken of the foam over a range of superficial gas velocities in a solution of 10 ppm F150. The J_g 0.378, 0.708, 1.251 and 1.783 cm/s (Figure 6) are in the low foam stability regime: the images display the interface between the bubbly region and the foam as well as the foam surface. For the high foam stability cases, J_g 2.306, 2.819 and 3.321 cm/s, the images include the interface and the surface (Figure 7).

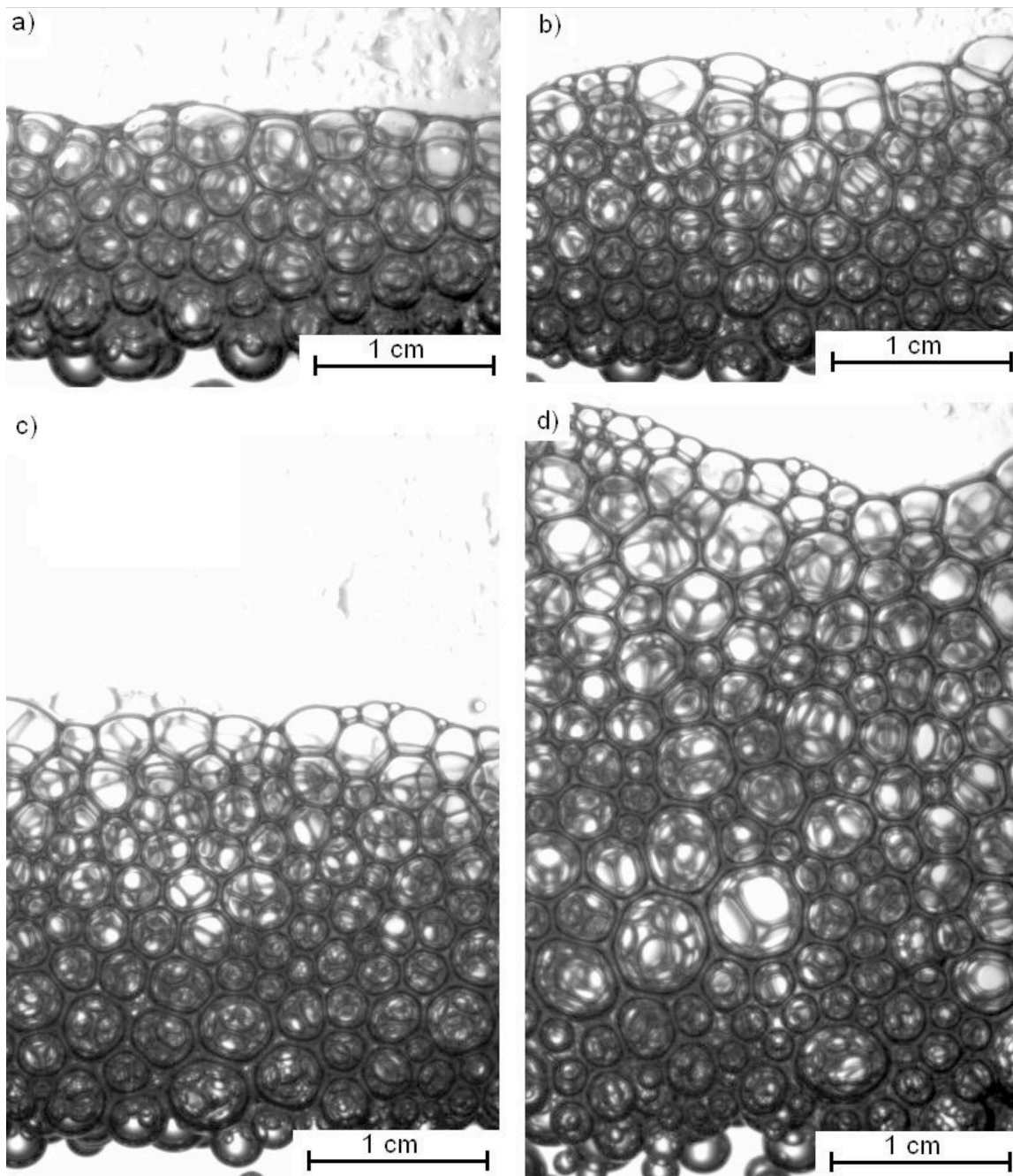


Figure 6: Images of foam formed with 10 ppm F150 at different superficial gas velocities: a) 0.378 cm/s ; b) 0.708 cm/s ; c) 1.251 cm/s ; d) 1.783 cm/s.

Figure 6 features spherical foam bubbles with thick films. The bubbles remain spherical from the interface up to the surface of the foam. It is at the surface of the foam that bubble shape becomes polyhedral. Upon arrival at the surface of the foam,

it appears that drainage is accelerated. The films between two bubbles are visible and are in the range 0.5 to 1 mm (i.e., within the hydrodynamic interaction stage).

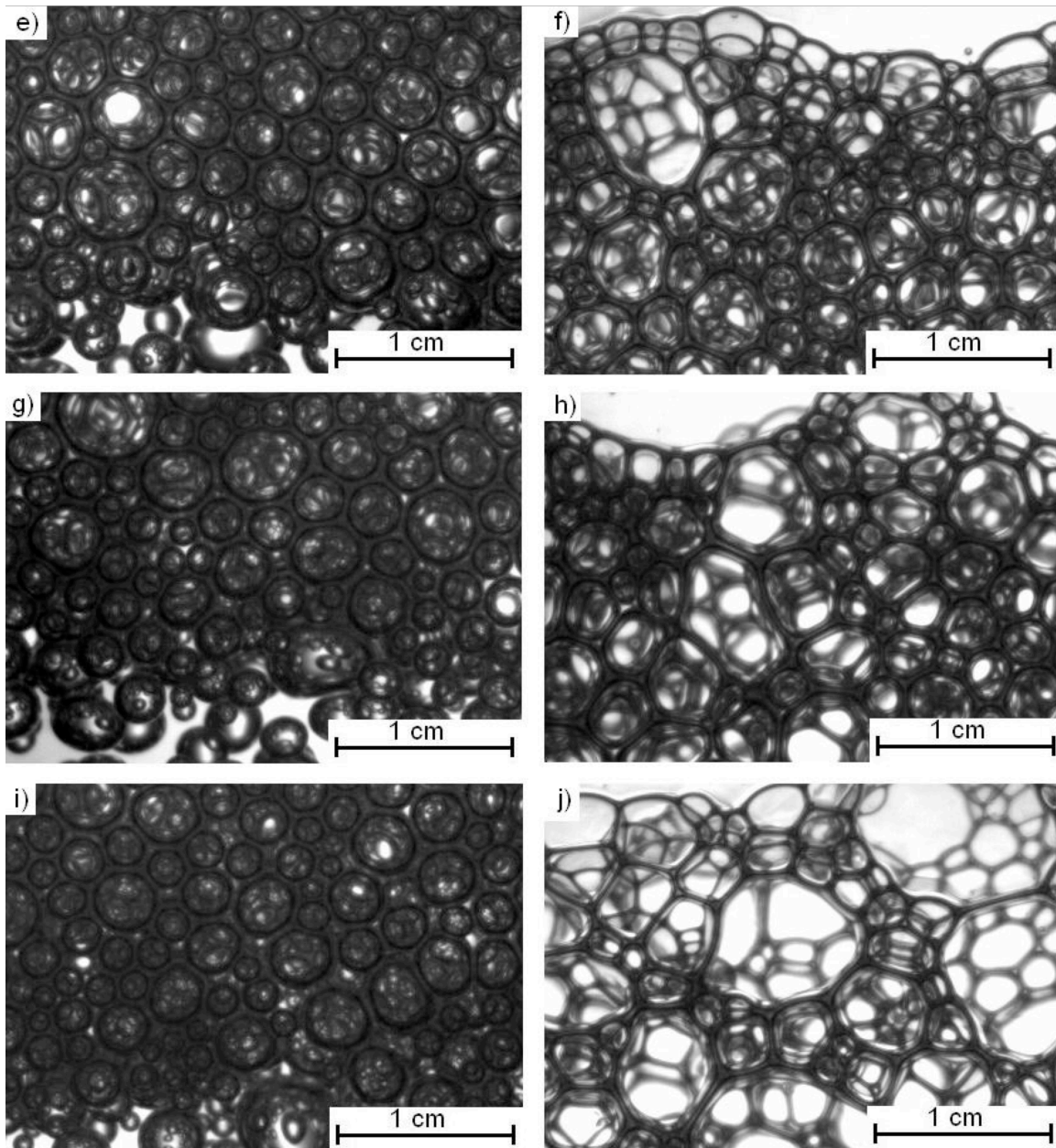


Figure 7: Image of foam formed with 10 ppm F150 at different superficial gas velocities: e) at the interface 2.306 cm/s ; f) at the surface 2.306 cm/s ; g) at the interface 2.819 cm/s ; h) at the surface 2.819 cm/s ; i) at the interface 3.321 cm/s ; j) at the surface 3.321 cm/s.

In the high stability regime the foam exhibits a different structure from the low stability foam in both the interface region and the surface. At the interface of the high stability

foam (Figure 7: e,g,i), the films are much thicker than the films of the low stability bubbles. Also, the bubbles are spherical and are seldom distorted by neighbouring bubbles. At the surface of the high stability foam (Figure 7: f,h,j), the bubbles are larger than below, indicating coalescence takes place within the foam. Besides their larger diameter, the high stability foam surface bubbles are polyhedral in shape. The films, although thinner than at the bubbly region/foam interface, are still visible and thicker than one might expect knowing coalescence is occurring.

A qualitative observation is that none of the films appear to be uniform in thickness; i.e., around a single bubble there can be a thick film and a thin film. This non-uniformity of film thickness suggests that a bubble can coalesce with its neighbour, as their separating film reaches a critical rupture thickness, while the film on the opposite side remains thick.

Liquid Fraction of Foam and Bubbly Region

For all conditions the hydrostatic pressure profiles were taken for both the bubbly region and the foam region (see Figure 8 for examples of pressure profiles) and gas holdup was determined. It was found that the pressure profiles were linear when there was sufficient depth to establish the trend reliably (i.e., in the bubbly zone and in the foam when sufficiently deep). This observation has been made by others (Ireland and Jameson, 2007). In cases where the foam was too shallow, the pressure was measured at the interface between the bubbly and foam zones. The foam height was measured with high precision (± 0.01 mm) and the two pressure readings (at the top of the foam and the

foam interface) were used to estimate $\Delta P / \Delta y$. This approach assumes that the pressure profile remains linear in shallow foams as it proved to be in deep foams.

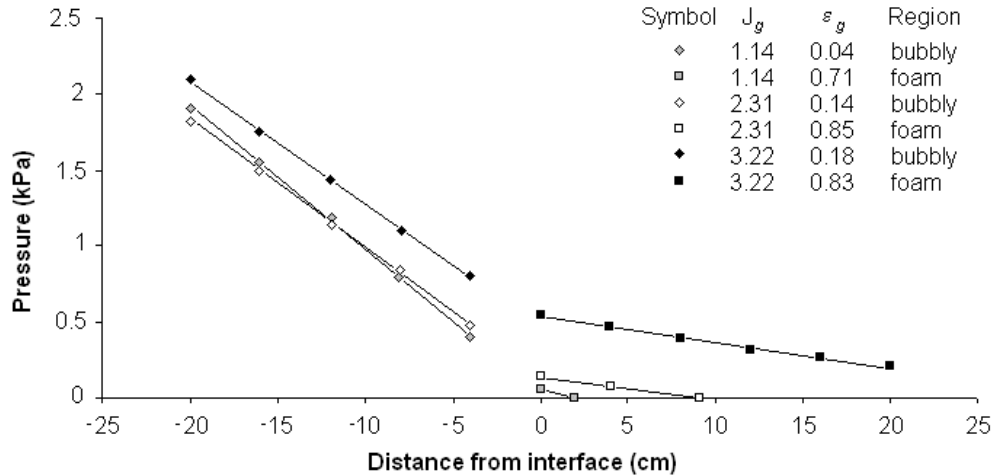


Figure 8: Hydrostatic pressure profiles used to calculate gas holdup of bubbly zone and foam zone of systems at different superficial gas velocity, J_g . All examples taken from the 10 ppm F150 case

Figure 9 shows the gas holdup for 1, 10, 50 ppm solutions of F150 for J_g up to values just below flooding. The gas holdup linearly increased with J_g , in accordance with past studies (Xu et al., 1991). The gas holdup for the foam region that corresponds to the regime of low foam stability is between the gas holdup of the bubbly zone and approximately a (fractional) gas holdup of 0.7. This would be the region where bubbles remain spherical and hydrodynamic forces dominate foam stability. As mentioned, point contact between bubbles does not take place until a gas holdup of approximately 0.74. The change from low to high stability foam may have its origin in the forces involved: Below ε_g 0.74, stability is due to hydrodynamic forces, while above 0.74, hydrodynamic forces progressively give way to physiochemical forces. Table 2 demonstrates how foam stability derived from physiochemical forces is orders of magnitude greater than foams stabilized by hydrodynamic forces alone.

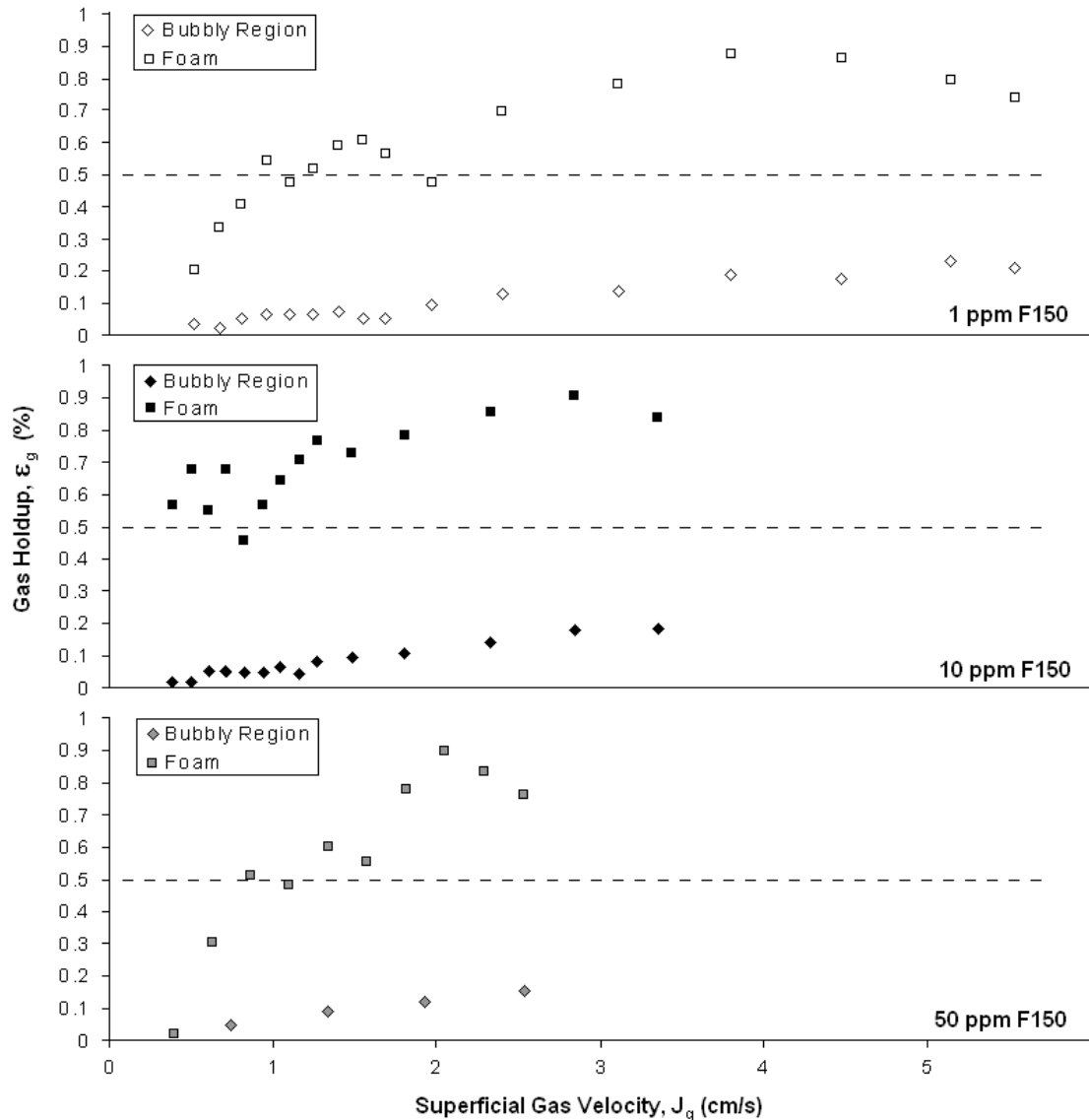


Figure 9: Gas holdup in bubbly and foam zones for 1, 10 and 50 ppm F150 solutions.

There is a maximum in gas holdup of the foam at approximately 0.9. The superficial gas velocity at which this maximum is reached seems to have a link to the concentration of the frother: The maximum occurs at ca. 4 cm/s, 3 cm/s and 2 cm/s for 1, 10 and 50 ppm, respectively. Continued increase in superficial gas velocity above the maximum sees the gas holdup drop. This reflects increased water being entrained into the foam by the bubbles entering from the bubbly region.

It is important to note that the lowest liquid fraction measured in the foam was approximately 10%. Many current foam models, have an upper liquid fraction ca. 10 vol%, and may not, therefore, be appropriate to model foams formed with frothers.

DISCUSSION

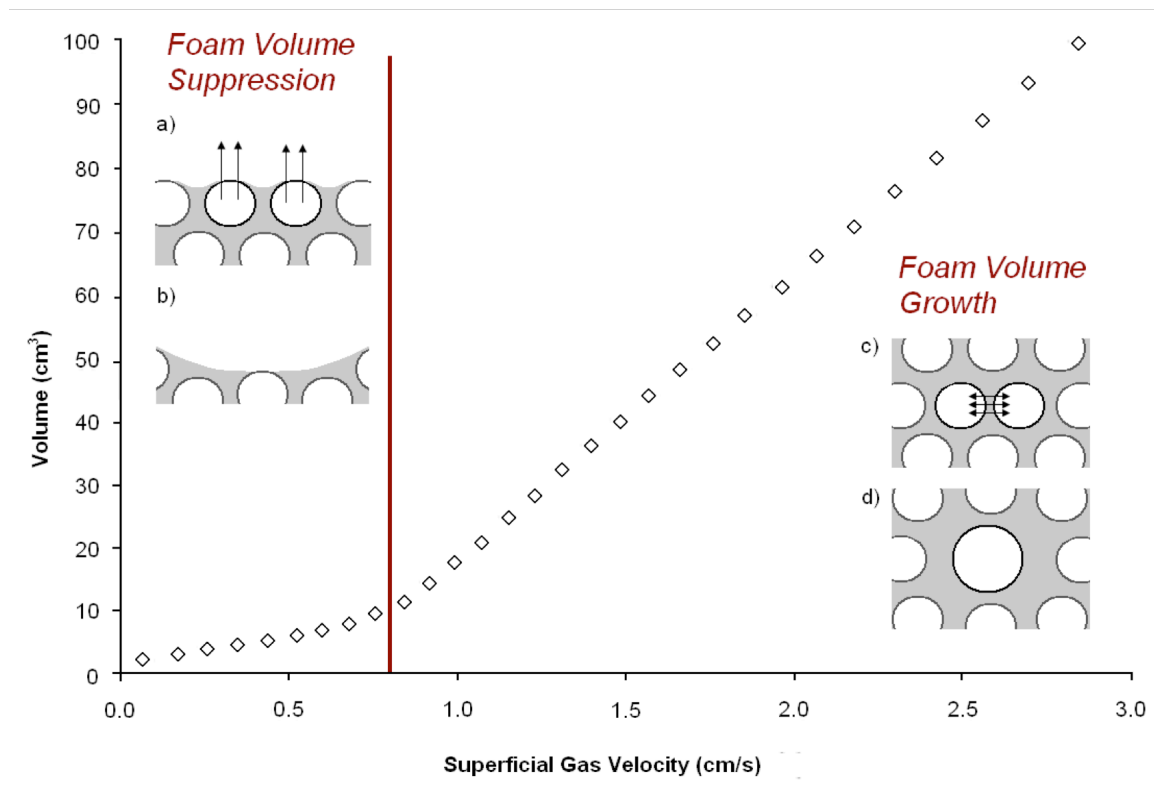


Figure 10: The regions of foam stability due to the fixed area vessel's geometry. Foam volume suppression occurs when too many bubbles are exposed to the foam surface (a) and air escapes the foam (b). Foam volume growth occurs when bubbles have formed films sufficiently thin for rupture and there is not enough foam surface available to allow escape of the ruptured bubbles (c). The consequence is that many bubbles coalesce with their neighbours and form larger bubbles (d).

Evidence suggests that foam stability is influenced by the vessel geometry (Figure 10). In a fixed cross-section area container (e.g. cylinder) at low J_g , foam volume experiences a suppression effect due to an excess of surface area. The result is that gas escapes the

surface prematurely (Figure 10, b). At high J_g , foam volume grows due a deficit of surface area compared to the number of bubbles arriving. Bubble films in the foam thin to the point of rupture, but due to lack of access to the foam surface, this means coalescence occurs and the resulting bubble remains within the foam (Figure 10, d).

CONCLUSIONS

A fixed area column was used to measure foam stability of F150 as a function of superficial gas velocity (J_g). Two foam stability regimes were observed. Low stability was associated with low J_g , stability increased by a factor of 10 at high J_g . Images of the low stability foam showed that inter-bubble film was thick with the sole exception of the foam surface bubbles. Images of the high foam stability regime showed evidence of coalescence within the foam. The lowest liquid fraction measured was approximately 10%.

The stability difference is due to the geometry of the vessel. The observed regimes of foam suppression at low gas flowrates and foam growth at high gas flowrates appear to be an interaction between bubble size (diameter) and the bubbly region/foam interfacial area. The role of surfactant becomes difficult to measure when cell geometry affects the amount of foam volume produced.

REFERENCES

- BARBIAN, N., VENTURA-MEDINA, E. & CILLIERS, J. J. 2003. Dynamic froth Stability in froth flotation. *Minerals Engineering*, 16, 1111-1116.
- BIKERMAN, J. J. 1938. The unit of foaminess. *Transactions of the Faraday Society*, 34, 634 -638.
- BIKERMAN, J. J. 1973. *Foams*, New York, Springer-Verlag.

- COX, S. J., WEAIRE, D., HUTZLER, S., MURPHY, J., PHELAN, R. & VERBIST, G. 2000. Applications and Generalizations of the Foam Drainage Equation. *Proceedings: Mathematical, Physical and Engineering Sciences*, 456, 2441-2464.
- CUTTING, G. W., WATSON, D., WHITEHEAD, A. & BARBER, S. P. 1981. Froth structure in continuous flotation cells: Relation to the prediction of plant performance from laboratory data using process models. *International Journal of Mineral Processing*, 7, 347-369.
- CZARNECKI, J., MALYSA, K. & POMIANOWSKI, A. 1982. Dynamic Frothability Index. *Journal of Colloid and Interface Science*, 86.
- DERJAGUIN, B. & LANDAU, L. 1941. A theory of the stability of strongly charged lyophobic sols and the coalescence of strongly charged particles in electrolytic solution. *Acta Phys.-Chim. USSR*, 14, 633-662.
- GÉLINAS, S., FINCH, J. & GOUET-KAPLAN, M. 2005. Comparative real-time characterization of frother bubble thin films. *Journal of colloid and interface science*, 291, 187-191.
- GUPTA, A. K., BANERJEE, P. K., MISHRA, A., SATISH, P. & PRADIP 2007. Effect of alcohol and polyglycol ether frothers on foam stability, bubble size and coal flotation. *International Journal of Mineral Processing*, 82, 126 - 137.
- HAAS, P. A. & JOHNSON, H. F. 2002. A Model and Experimental Results for Drainage of Solution between Foam Bubbles. *Industrial & Engineering Chemistry Fundamentals*, 6, 225-233.
- IRELAND, P. M. & JAMESON, G. J. 2007. Liquid transport in a multi-layer froth. *Journal of Colloid and Interface Science*, 314, 207-213.
- IVANOV, I. 1980. Effect of surface mobility on the dynamic behavior of thin liquid films. *Pure Appl. Chem*, 52, 1241-1262.
- KANN, K. & FEKLISTOV, V. 1977. *Izv. Sib. Otd. AN USSR Ser. Tech.*, 2, 116.
- KOEHLER, S. A., HILGENFELDT, S. & STONE, H. A. 2000. A generalized view of foam Drainage: Experiment and Theory. *Langmuir*, 16, 6327-6341.
- LASKOWSKI, J. S., TLHONE, T., WILLIAMS, P. & DING, K. 2003. Fundamental properties of the polyoxypropylene alkyl ether floatation frothers. *International Journal of Mineral Processing*, 72, 289 - 299.
- MALYSA, K., COHEN, R., EXEROWA, D. & POMIANOWSKI, A. 1981. Steady-state foaming and the properties of thin liquid films from aqueous alcohol solutions. *Journal of Colloid and Interface Science*, 80, 1-6.
- NEETHLING, S., LEE, H. & CILLIERS, J. 2002. A foam drainage equation generalized for all liquid contents. *Journal of Physics: Condensed Matter*, 14, 331-342.
- OVERBEEK, J. 1941. *Theorie der electrophorese: het relaxatie-effect*, HJ Paris.
- PUGH, R. 1996. Foaming, foam films, antifoaming and defoaming. *Advances in Colloid and Interface Science*, 64, 67-142.
- SAFOUANE, M., SAINT-JAMES, A., BERGERON, V. & LANGEVIN, D. 2006. Viscosity effects in foam drainage: Newtonian and non-newtonian foaming fluids. *The European Physical Journal E: Soft Matter and Biological Physics*, 19, 195-202.
- VERWEY, E. 1947. Theory of the Stability of Lyophobic Colloids. *The Journal of Physical Chemistry*, 51, 631-636.

- VERWEY, E. J. W. & OVERBEEK, J. Th. G.(1948) Theory of the stability of lyophobic colloids. *Elsevier Publ. Co. Inc., London*, 8, 9.
- WANG, L. & YOON, R. 2008a. Effects of surface forces and film elasticity on foam stability. *International Journal of Mineral Processing*, 85, 101-110.
- WANG, L. & YOON, R.-H. 2008b. Effects of surface forces and film elasticity on foam stability. *International Journal of Mineral Processing*, 85, 101-110.
- XU, M., FINCH, J. A. & URIBE-SALAS, A. 1991. Maximum gas and bubble surface rates in flotation columns. *International Journal of Mineral Processing*, 32, 233-250.
- YIANATOS, J. B., FINCH, J. A. & LAPLANTE, A. R. 1986. Holdup profile and bubble size distribution of flotation column froths. *Canadian Metallurgical Quarterly*, 25, 23-29.

CHAPTER 2:

FOAM VOLUME MEASUREMENTS WITH A VARIABLE AREA VESSEL

INTRODUCTION

Fixed area vessels (such as columns) have an effect on the foam volume generated. The observed regimes of foam suppression at low gas flowrates and foam growth at high gas flowrates appear to be an interaction between bubble size (diameter) and the bubbly region/foam interfacial area. The role of surfactant becomes difficult to measure when cell geometry affects the amount of foam volume produced.

Replacing the fixed area vessel with a variable area vessel can lessen the geometry bias. In addition to geometry, the hydrophobicity of the vessel walls has also been noted to have an effect (Papara et al., 2009). Any comparison of vessels must therefore use the same materials of construction. It should be noted from the outset that the total effect of the vessel cannot be completely removed only lessened.

WATKINS FUNNEL: BACKGROUND THEORY

Watkins (1973) developed a variable area vessel for dynamic foam volume measurements. His research was driven by the observation (testing foaming of oils) that foam volume could quickly increase to a volume more than the test vessel could contain (referred to as “flooding”) upon a relatively small increase in gas flowrate. This is the very same effect observed in Chapter 1. Watkins looked at the foam system as the ability of a solution to retain air. The foam volume generated in a period of time was the difference between the air that entered the system and the air that exited namely,

$$V_f = \left(J_{g,B} A_{C,B} \right) dt - \left(J_{g,T} A_{C,T} \right) dt \quad (1)$$

where $J_{g,B}$ and $J_{g,T}$ are the superficial gas velocities at the bottom of the foam and the top of the foam, respectively, $A_{C,B}$ and $A_{C,T}$ are the cross sectional areas of the foam vessel at the bottom and the top and the bottom of the foam, respectively. Taking the derivative of the equation 1 gives:

$$\frac{\partial V_f}{\partial t} = J_{g,B} A_{C,B} - J_{g,T} A_{C,T} \quad (2)$$

that is, the volume of foam will either increase with time (when $J_{g,B} A_B > J_{g,T} A_T$), decrease ($J_{g,B} A_B < J_{g,T} A_T$) or remain constant ($J_{g,B} A_B = J_{g,T} A_T$). At low gas flowrates, he argued, the area of the foam surface is greater than the equilibrium conditions can sustain and the rate of air escape from the foam surface is greater than the air arriving from the bubbly region and consequently the foam tends to collapse. At high gas flowrates, air loss from the surface is restricted by the limited area available and air now accumulates and drives the foam volume upward. With a fixed area vessel ($A_B = A_T$), such as columns, avoiding growth or suppression is difficult.

Watkins's proposed a conical vessel, the Watkins Funnel. He tested various cone angles and found that reproducibility improved from 30° to 60° but measurements became difficult to make above 60°. The Watkins Funnel has been adopted in foam research using an internal angle of 60° (Ross and Suzin, 1985, Waltermo et al., 1996, Tarkan and Finch, 2005).

PYSIOCHEMICAL/KINEMATIC REGIMES: BACKGROUND THEORY

It was seen in a fixed area vessel that there were two stability regimes. In the variable

area Watkins Funnel, two stability regimes are also observed (Ross and Suzin, 1985, Waltermo et al., 1996). Ross and Suzin provide an explanation based on D'yakonov (1942) that the two regimes are due to a change in the kinetics of the bubbly region. If a sufficiently large gas flowrate range is used two foam stability regimes become apparent (Dyakonov, 1942). The regime at low gas rate is dominated by physiochemical conditions, i.e., the properties due to surfactant. The high gas rate regime is influenced by kinematic conditions as well as physiochemical properties. In other words, the high gas flowrate regime exhibits different stability due to the kinetic nature of the bubbly zone.

There are two known phenomena in flotation literature that support this observation. The first is increased water entrainment into foam at high gas flowrates (Finch et al., 1989). The second is the bubble coalescence in the foam close to the bubbly zone/foam interface due to the kinetic energy imparted by the decelerating air bubbles entering the foam (Ata et al., 2003, Yianatos et al., 1986).

From his analysis, D'yakonov derived the following:

$$\frac{h_f}{J_g \tau} = b(\text{Re})^m \left(\frac{H}{d} \right)^p \quad (3)$$

where h_f is foam height (m), J_g is the superficial gas velocity (Q/A_c) (m/s), τ is a measure of the solution's intrinsic ability to form stable foam (s), H is the height of the solution from the bottom of the column to the foam-liquid interface (m), and m and p are empirical exponents and Re is the Reynolds number defined by $J_g d / \nu$, where ν is the kinematic viscosity (ratio of dynamic viscosity to density) of the solution (m^2/s), and d is

the hydraulic diameter of the apparatus (m) ($d = (4 \times \text{Area of column}) / \text{wetted perimeter of column}$). D'yakanov found that at high Reynolds numbers ($Re > 100$) the foam height is influenced by the kinematic conditions, but for $Re < 100$ kinematic conditions did not contribute to dynamic foam stability ($m = 0$). Foam stability in this low Re region was determined by cell geometry (such as the hydraulic diameter, d) and by the intrinsic foaminess of the solution (represented as τ).

Ross and Suzin, reflecting on D'yakanov's work, proposed that the constant b contains a measure of the amount of bubble surface area entering the froth, a value determined by gas flowrate and bubble size in the bubbly region. Bikerman (1973) pointed out that the influence of solution height on foam height (the H term in equation 3) is marginal with sufficient solution height and should only be considered a factor in foam stability when the lack of solution noticeably limits equilibrium foam height. Regardless, D'yakanov's work indicates that tests to isolate the value τ for a particular surfactant must consider the effect that gas rate has on the bubbly zone. It would seem that to test for intrinsic foaminess low gas flowrates should be used.

EXPERIMENTAL

Foaming Vessel

The conical vessel was made of glass, with r_0 1.09 cm and cone angle (θ) of 60° (Figure 3). Air bubbles were produced by a coarse glass frit (nominal pore size 40 – 60 μm) with surface area 3.74 cm^2 and distance from the frit to foam base 5 cm. The gas flowrate range was 0.2 ml/s to 10.5 ml/s. Gas flowrates were randomized.

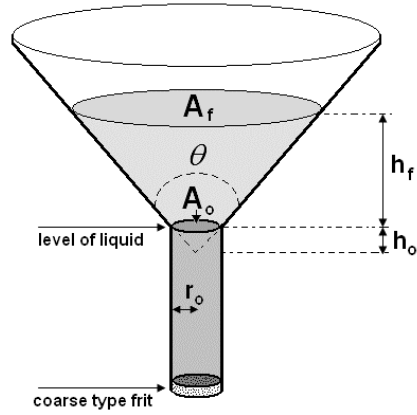


Figure 1: Conical foam test apparatus schematic with nomenclature

Foam volume in the conical vessel was calculated from the following expression (see Figure 1):

$$V_f = \left(\frac{1}{(3\pi)^{1/2}} \right) A_f^{3/2} - \left(\frac{h_o A_o}{3} \right) \quad (4)$$

where A_o is cross sectional area of the cylindrical bubbly zone of the vessel, h_o is a function of the cylindrical radius (r_o) and the cone angle (θ) and A_f is represented by the following equation:

$$A_f = \pi \tan(\theta/2)^2 (h_f + h_o)^2 \quad (5)$$

where h_f is the distance from the foam surface to the interface (i.e., foam height).

The vessel is rinsed with the solution to be tested before being filled with 19.51 ml (+/- 0.01 ml) of the test solution. After every test, the vessel was rinsed with acetone and distilled water. Before a new set of experiments and at the slightest sign of contamination, all glassware was cleaned with chromic acid to ensure the hydrophobicity of the vessel remained constant.

Foam Volume Measurement

A TSPC-30S1-232 ToughSonic® PC ultrasonic sensor was used to measure the distance from the surface of the foam to the sensor. The corresponding foam volume was estimated from a calibration of volume vs. height. Three hundred height measurements were taken for each gas flowrate tested. Volume measurements had a precision of 0.05 cm³.

Surfactants

The surfactants used were three commercial flotation frothers F150, FX 160-05 and MIBC (Table 1). Every concentration was replicated three times and the precision of concentration was 0.003%.

Table 1- Frothers used in foam volume experiments

Frother Type	Description	Molecular Weight (g/mol)	Chemical Formula
F150	Polypropylene glycol	425	H-(C ₃ H ₆ O) ₇ -OH
FX 160-05	Polypropylene glycol alkyl ether	205	CH ₃ CH ₂ CH ₂ (C ₃ H ₆ O) _{2,5} -OH
MIBC	Methyl isobutyl carbinol	102	CH ₃ CHCH ₃ CH(OH)CH ₃

Temperature of the solution was measured prior to and after every test and was constant at 19.25 °C (± 0.05 °C).

RESULTS

Hysteresis

The gas flowrate was increased in approximately $0.3 \text{ cm}^3/\text{s}$ increments from $0.43 \text{ cm}^3/\text{s}$ to $10.06 \text{ cm}^3/\text{s}$ then decreased in like manner. The objective was to reveal any effect on foam volume of the order with which the experiment is conducted.

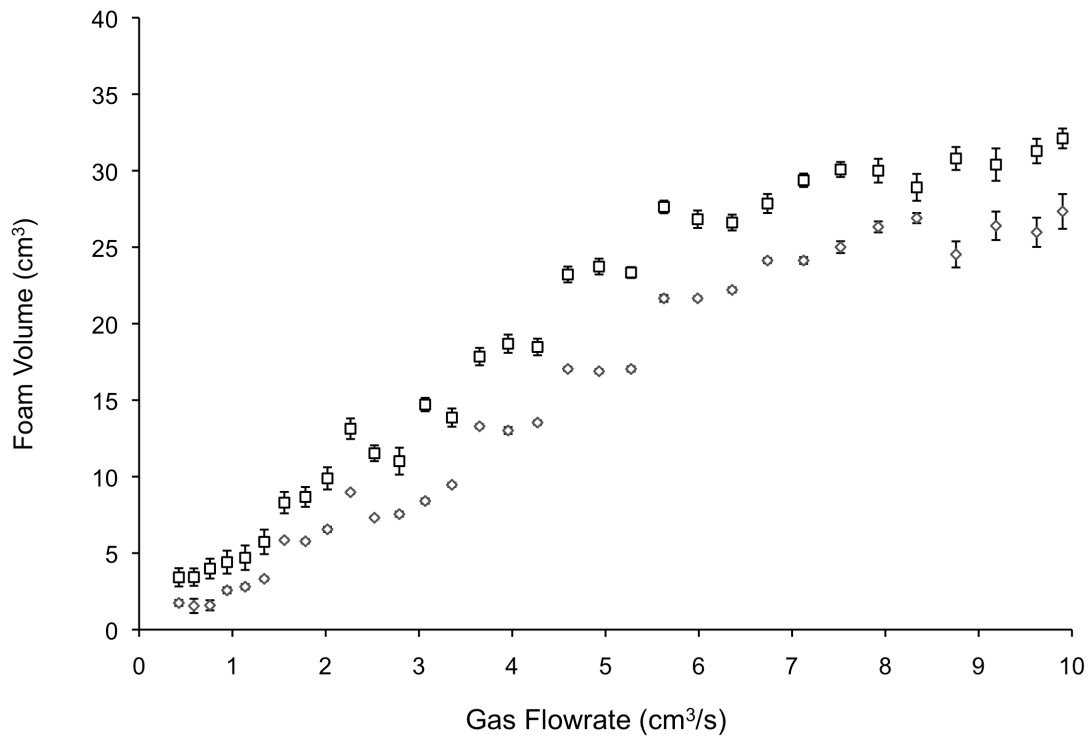


Figure 11: Hysteresis loop of the conical vessel: (◇) represents increasing gas flowrate; (□) represents decreasing gas flowrate.

Figure 2 reveals a hysteresis loop in foam volume versus gas flowrate, showing that for every flowrate the foam volume is greater in the decreasing case than in the increasing case. The increased foam volume (increased stability) in decreasing loop is likely due to greater film thickness at the start, i.e., at $10.06 \text{ cm}^3/\text{s}$. The amount of water that accumulates in the foam steadily increases on the increasing part of the loop being

entrained with the bubbles from the bubbly zone. Once in the foam, the bulk viscosity forces slow water drainage from the films. Upon decreasing the gas flowrate, this accumulated water thus provides additional initial foam stability. The phenomenon is similar to the increased foam stability that is observed when wash water is injected into the top of a foam (Yianatos et al., 1986, Tao et al., 2000). The two strategies to handle this effect are either to study as a hysteresis loop or to randomize the gas flowrates used so that the effect is minimized. Studying as the loop may have merit (a loose analogy is the value in studying hysteresis in a material's magnetization) but the strategy adopted here is the randomization of gas flowrates. For each concentration, three repeat solutions were prepared and each was measured with a different random order of gas flowrates.

Low/High Gas Flowrate Regime Transition

The transition value was identified by using a linear transition model (Bacon and Watts, 1971) represented in the following equation:

$$Y = \alpha_0 + \alpha_1(\chi - \chi_0) + \alpha_2(\chi - \chi_0)\tanh\{(\chi - \chi_0)/\gamma\} \quad (6)$$

where χ_0 represents the gas flowrate at which the transition occurs. The term $\tanh\{(\chi - \chi_0)/\gamma\}$ is the transition function and varies between -1 and +1 when below and above the χ_0 value, respectively. The γ is a parameter that moderates the transition from one slope value to the next (i.e., when transition occurs over a period). The γ parameter was maintained at 1 for a moderate transition. Foam stability in the low gas flowrate regime is determined as $\alpha_1 - \alpha_2$ and for the high gas flowrate regime as $\alpha_1 + \alpha_2$. The equation was fitted to the data through a minimization of the sum of squares routine. Both regions are treated as linear even though the higher gas regime is predicted to be

exponential in the D'yakonov equation. Ross and Suzin (1985) did not observe the exponential trend in their data either and attributed it to the gas flowrate remaining below the level necessary to initiate exponential growth using superficial gas velocity up to 0.27 cm/s. Waltermo et al. (1996) tested a greater range of gas velocity (J_g to 2.7 cm/s) and the data still did not show exponential behaviour but remained linear.

Foam Stability

Equation 6 was successfully fitted to the data. Figure 3 shows two examples obtained from a 1 ppm F150 solution and a 10 ppm F150 solution. Examining the latter, one can see that data are not smooth but oscillate about the average trend due to the hysteresis effect. Nevertheless there is a clear transition at ca. $1.5 \text{ cm}^3/\text{s}$. In contrast, the 1 ppm F150 data demonstrate no marked transition.

Table 2 shows the results for the three frothers. The Table gives the average parameter values for each concentration and frother. The parameter χ_o is the transition gas flowrate. Transition is not sharp; rather it takes place over ca. $2 \text{ cm}^3/\text{s}$.

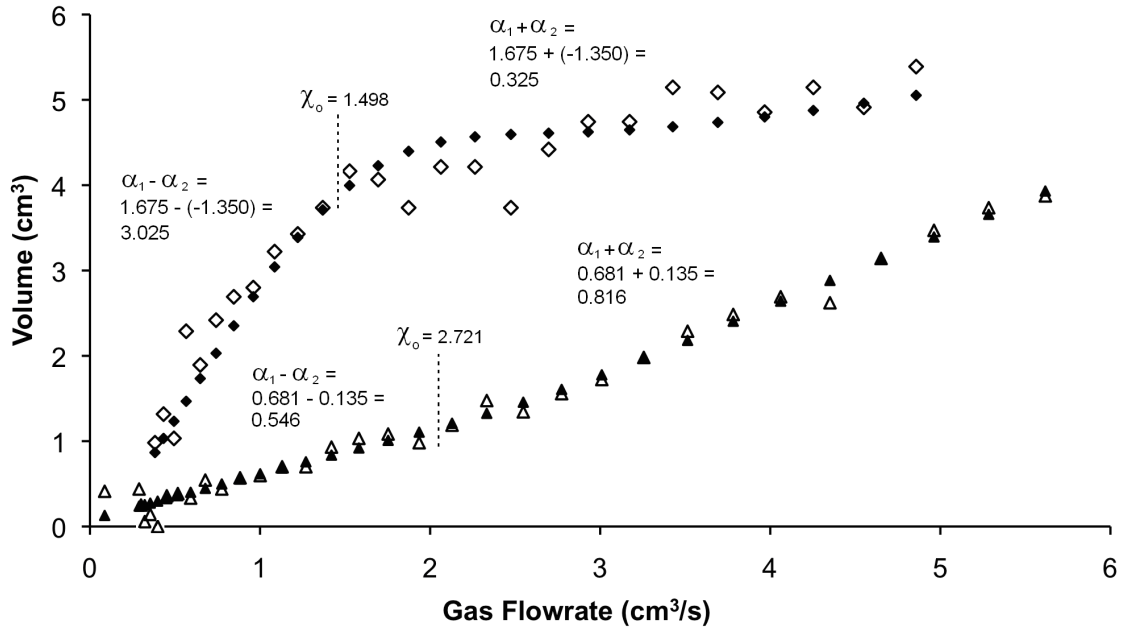


Figure 12: Example of equation 6 being fit to both a 1ppm F150 and 10ppm F150 data set. (Δ , \diamond) represents 1 ppm F150 and 10 ppm F150 data respectively. (\blacktriangle , \blacklozenge) represents the fitted equation 6 curve for 1 ppm F150 and 10 ppm F150 respectively.

Table 2 - Transition Gas Flowrate values (χ_0) and the foam stability for region below the transition ($\alpha_1 - \alpha_2$) and above ($\alpha_1 + \alpha_2$).

	Concentration (ppm)	χ_0 (cm ³ /s)	α_1	α_2	$\alpha_1 - \alpha_2$	$\alpha_1 + \alpha_2$
					Lower Σ (s)	Upper Σ (s)
F150	1	2.400	0.668	0.068	0.600	0.737
	3	1.899	1.560	-0.733	2.293	0.827
	10	1.117	2.107	-1.364	3.471	0.743
	30	5.557	3.231	-1.261	4.492	1.970
	100	4.197	4.739	-1.273	6.012	3.465
	300	4.682	4.070	-0.296	4.367	3.774
FX 160-05	3	2.743	0.934	-0.167	1.101	0.767
	10	6.433	1.552	-1.325	2.877	1.762
	30	5.970	4.917	-0.911	5.828	4.006
	100	6.242	4.659	-0.756	5.415	3.903
	300	3.375	5.229	-0.670	5.899	4.558
	1000	4.096	4.440	-1.420	5.860	3.019
MIBC	10	4.076	0.578	-0.143	0.721	0.435
	30	4.269	2.394	0.397	1.997	2.791
	100	4.012	4.666	-0.194	4.860	4.472
	1000	5.590	5.584	-1.338	6.922	4.246
	3000	5.523	5.347	-1.792	7.139	3.556
	10000	5.169	4.600	-1.800	6.400	2.800

Transition Gas Flowrate

D'yakonov (1942) predicted that transition would take place around a Reynolds number of 100. Assuming that the dynamic viscosity remains unchanged with the amount of frother added and the hydraulic radius corresponds to the bubbly zone / foam interface, a Reynolds number of 100 would occur at $1.72 \text{ cm}^3/\text{s}$. Figure 4 shows the transition values for all the tested conditions. With the exception of 10 ppm F150 all transitions occur at values greater than Re 100. Since D'yakonov used a fixed area column with diameter 40 mm and recalling the findings of Chapter 1, the sensitivity to the gas flowrate he witnessed at Re 100 was more likely due to a geometry effect of the test vessel.

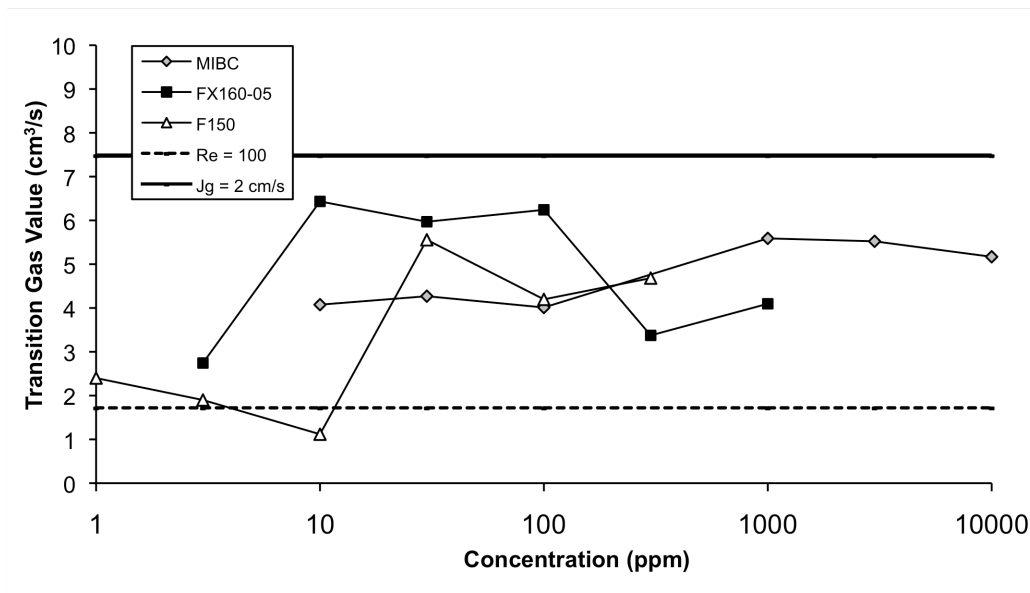


Figure 13: Transition gas flowrate values determined for MIBC, FX 160-05 and F150.

There is no apparent relation between the transition value and frother concentration or frother type (Figure 4). Values vary between 2 and $6 \text{ cm}^3/\text{s}$. Figure 4 illustrates that while there is a transition gas flowrate it does not readily correlate with a frother's surfactant properties.

In a test with tracer injected into the bubbly region, Finch et al. (1989) found that above a superficial gas velocity of 2 cm/s there was significant entrainment of bubbly zone water into the foam. A J_g of 2 cm/s occurs at 7.48 cm³/s, indicated on Figure 4. The transition values occur at lower gas flowrate values than this high-end entrainment gas flowrate. The change in foam stability at high gas flowrates may, nevertheless, be due to the increased amount of water entrained with the bubbles entering the foam.

Foam Stability at High/Low Gas Flowrates

Figure 5 shows the stability of foam above and below the gas flowrate transition value. With all three frothers tested, it is noted with increasing concentration that there is a region of increasing stability followed by a region of constant stability and then a region of decreasing stability. This relationship was also observed in the study of frothers and foam behaviour by Tan et al. (2005b).

There is a marked difference between the stability associated with a low gas flowrate versus a high gas flowrate. Foams formed at low gas flowrates exhibit a higher stability than foams formed at high gas velocity. The known effect of high gas flowrate is increased entrainment (Finch et al., 1989) which would cause a thicker water film which, by itself, should increase foam stability. The origin of reduced foam stability lies in the same reason why entrainment increases, more bubbles entering the foam per unit time. There are two effects associated with bubbles arriving at the foam interface: the bubble pushes liquid (solution) from the bubbly zone into the foam; and the bubble kinetic energy is transferred into the foam as it decelerates. The latter effect appears to dominate

at high gas flowrates. Coalescence has been observed directly above a froth interface at high gas rates (Yianatos et al., 1986).

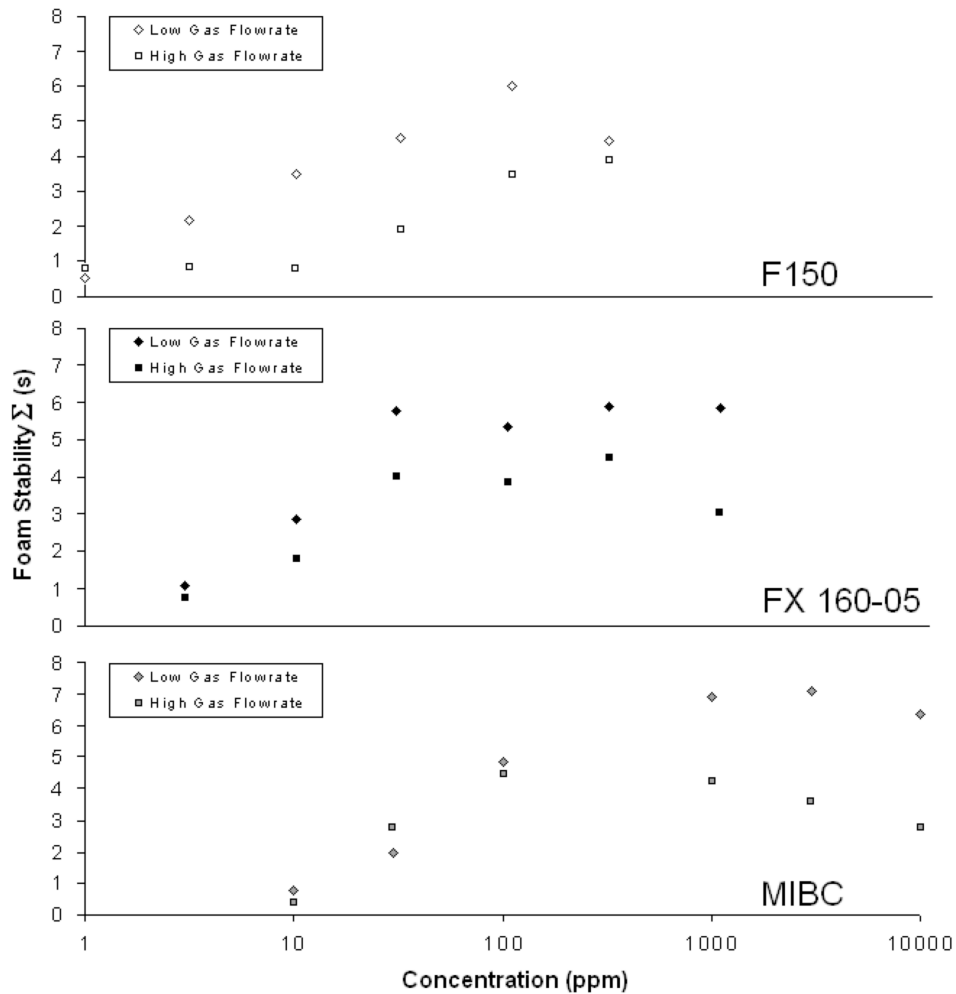


Figure 14: Foam stability (s) for ranges of gas flowrates below and above the transition gas flowrate value (noted a low and high gas flowrate respectfully). Frothers F150, FX 160-05 and MIBC are tested over a range of concentrations.

As the bubble expands in a foam, surface tension gradients occur between the region of the bubble in contact with the Plateau border and the region located in the lamellar film. This surface tension difference drives the transport of bulk solution into the thinning film, resulting in a stabilizing force (Tan et al., 2005a). The mechanism, known as the Gibbs-Marangoni effect, is noted to have a strong link to surfactant concentration (Figure 6).

Pugh (1996) explains that if frother concentration is too low, no significant surface tension gradients exist and the film ruptures. At high frother concentration (the solubility limit of the frother has been exceeded), surface concentration is maintained constant due to diffusion of frother from the bulk solution and no surface tension gradients exist and, again, the film ruptures. There is a concentration range in which surface tension gradients are high enough to cause film restoration.

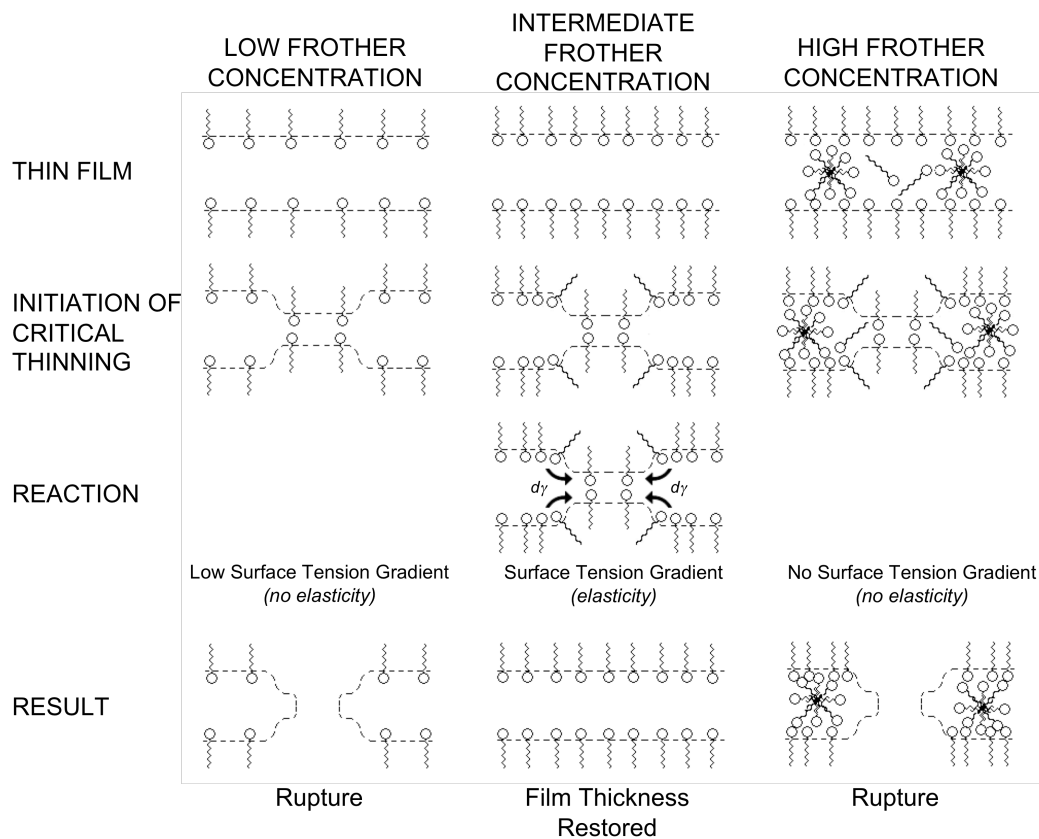


Figure 15: Frother concentration effect on the Gibbs-Marangoni film elasticity. Low concentration films do not develop sufficient surface tension gradients to counter film drainage. At high concentration films again fail to generate sufficient gradients due concentration differences being countered by fast bulk diffusion. There exists a range of concentration that exhibits maximum surface tension gradients.

Referring the Figure 5, the Gibbs-Marangoni effect is a stabilizing mechanism at both low and high gas flowrate regimes. For all three frothers, the concentration stability regions occur at different concentrations for the low and high gas regimes. For F150 at

300 ppm stability is entering the decreasing trend at low gas flowrate while the high gas regime is still in the increasing stability regime. For MIBC and FX 160-05 stability in the high gas regime begins to decrease before that for the low gas regime stability.

CONCLUSIONS

The Watkins Funnel was used to test the effect of frother type and concentration on foam stability. In relation to gas flowrate, two stability regimes were identifiable. The gas flowrate associated with transition varied between 2 and 6 cm³/s and had no readily apparent relation to frother type or concentration. Foam stability exhibited a high stability over a mid-range of frother concentration, a result explained by the Gibbs-Marangoni effect. There is some evidence that the concentration range of maximum stability is different for the low gas flowrate regime versus the high gas flowrate regime. The high gas regime showed consistently lower stability than the low gas regime at all concentrations. This stability decrease is contrary to what is seen in a fixed area vessel. The decrease in stability at high gas flowrates appears to be due to an increase in turbulence in the bubbly region.

REFERENCES

- ATA, S., AHMED, N. & JAMESON, G. J. 2003. A study of bubble coalescence in flotation froth. *International Journal of Mineral Processing*, 72, 255-266.
- BACON, D. W. & WATTS, D. G. 1971. Estimating the transition between two intersecting straight lines. *Biometrika*, 58, 525-534.
- BIKERMAN, J. J. 1973. *Foams*, New York, Springer-Verlag.
- DYAKONOV, G. K. 1942. Application of the theory of similarity to the study of the process of foam formation. *Journal of Technical Physics (U.S.S.R.)*, 12, 302 - 314.
- FINCH, J., YIANATOS, J. & DOBBY, G. 1989. Column froths. *Mineral Processing and Extractive Metallurgy Review*, 5, 281-305.
- PAPARA, M., ZABULIS, X. & KARAPANTSIOS, T. 2009. Container effects on the free drainage of wet foams. *Chemical Engineering Science*, 64, 1404-1415.

- PUGH, R. 1996. Foaming, foam films, antifoaming and defoaming. *Advances in Colloid and Interface Science*, 64, 67-142.
- ROSS, S. & SUZIN, Y. 1985. Measurement of Dynamic Foam Stability. *Langmuir*, 1, 145-149.
- TAN, S., FORNASIERO, D., SEDEV, R. & RALSTON, J. 2005a. Marangoni effects in aqueous polypropylene glycol foams. *Journal of colloid and interface science*, 286, 719-729.
- TAN, S., FORNASIERO, D., SEDEV, R. & RALSTON, J. 2005b. The role of surfactant structure on foam behaviour. *Colloids and Surfaces A: Physicochemical and Engineering Aspects*, 263, 233-238.
- TAO, D., LUTTRELL, G. & YOON, R. 2000. A parametric study of froth stability and its effect on column flotation of fine particles. *International Journal of Mineral Processing*, 59, 25-43.
- TARKAN, H. & FINCH, J. 2005. Foaming properties of solvents for use in air-assisted solvent extraction. *Colloids and Surfaces A: Physicochemical and Engineering Aspects*, 264, 126-132.
- WALTERMO, A., CLAESSON, P., SIMONSSON, S., MANEV, E., JOHANSSON, I. & BERGERON, V. 1996. Foam and thin-liquid-film studies of alkyl glucoside systems. *Langmuir*, 12, 5271-5278.
- WATKINS, R. C. 1973. An improved foam test for lubricating oils. *Journal of the Institute of Petroleum*, 59, 106-113.
- YIANATOS, J. B., FINCH, J. A. & LAPLANTE, A. R. 1986. Holdup profile and bubble size distribution of flotation column froths. *Canadian Metallurgical Quarterly*, 25, 23-29.

CHAPTER 3:

COMPARISON OF A CONICAL VERSUS A CYLINDRICAL FOAMING VESSEL

INTRODUCTION

To differentiate the column and the cone as foaming vessels, all other features must be similar. The bubbling zone geometry, how the bubbles are produced and the size (diameter) of bubbles must be the same. By extension, this ensures that conditions at the interface between the bubbly zone and the foam are equal.

Two foaming vessels were constructed so that the only difference was the angle of inclination from the foam interface upwards (0° for the column and 60° for the conical vessel). The foam stability regimes for each vessel were indentified as well as their distinct foamability.

Since one goal is to better understand frother foaming properties, two frothers with known differences (MIBC and F150, which produce “dry” and “wet” foam, respectively) are used. Frothers are known for reducing bubble size by preventing coalescence (Ata et al., 2003). Therefore, to eliminate a change in bubble size as a factor in the foamability results, the minimum frother concentration used was above the critical coalescence concentration. Chapter 2 showed that there was a maximum foamability concentration, additional frother above this concentration resulting in a decreased foamability. The upper concentration giving maximum foamability was the upper limit used in this study.

THEORY

Figure 1 shows the general relationship between gas flowrate and foam volume for a fixed area vessel and a variable area vessel. A fixed area vessel (i.e., a column) exposes a limited area of foam surface, which either accelerates foam collapse (foam volume suppression) or constricts gas escape (foam volume growth). The collapse and growth regions are readily distinguishable at a transition gas flowrate, which may be a function of the column diameter. A large diameter column would have a wider range of gas flowrates in which foam volume is suppressed; i.e. higher transition gas flowrate. (As an aside, flotation cells have started to include a decreasing cross sectional area in their froth zone. The froth crowder, as it is commonly known, aids froth formation. Using Chapter 1 as a reference, the reduced cross sectional area provided by the crowder shifts conditions from foam volume suppression to foam volume growth.)

A variable area vessel equilibrates the amount of foam surface it exposes with the supply of bubbles. This simple expedient eliminates the foam suppression and growth regimes. Nonetheless, two regimes are evident in the gas flowrate / foam volume data. The foamability at low gas flowrates is greater (slope of foam volume vs. gas rate is higher) than that at high gas flowrates. The reason is not immediately clear but a tentative explanation is that turbulence in the bubbly region at high gas flowrates has a destabilizing effect. As gas flowrate is raised, bubbly zone kinetics increases which is dissipated in the foam. For this reason the two regimes in Figure 1 are referred to as low and high kinetic bubbly zones.

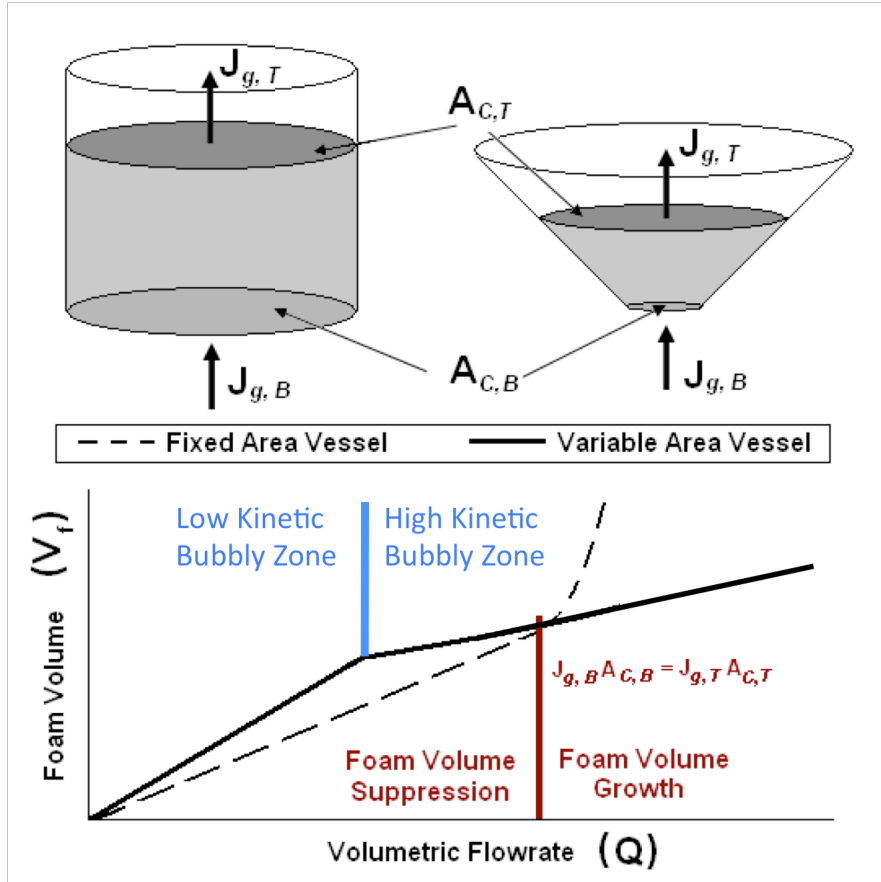


Figure 1: Foamability behavior in a fixed area vessel and a variable area vessel.

EXPERIMENTAL

Foaming Vessel

Two foaming vessels were used: a fixed-area column and a variable-area cone. The bubbly regions of both vessels are of equal in dimensions, material of construction (glass) and bubble generation (coarse glass frit (nominal pore size 40 – 60 μm)).

The cylindrical vessel was r_o 2.04 cm in diameter and 100 cm high with bubble generator of surface area of 3.27 cm^2 (Figure 2). The conical vessel was 2.18 cm with a cylindrical section 5 cm high and cone angle (θ) of 60° with bubble generator of surface area 3.74

cm² (Figure 2). The gas flowrate range was 0.2 ml/s to 10.5 ml/s. Gas flowrates were randomized.

The vessels are rinsed with the solution to be tested before being filled with 19.51 ml (+/- 0.01 ml) of the test solution. After every test, the vessels were rinsed with acetone and distilled water. Before a new set of experiments and at the slightest sign of contamination, all glassware was cleaned with chromic acid to ensure the hydrophobicity of the vessels remained constant.

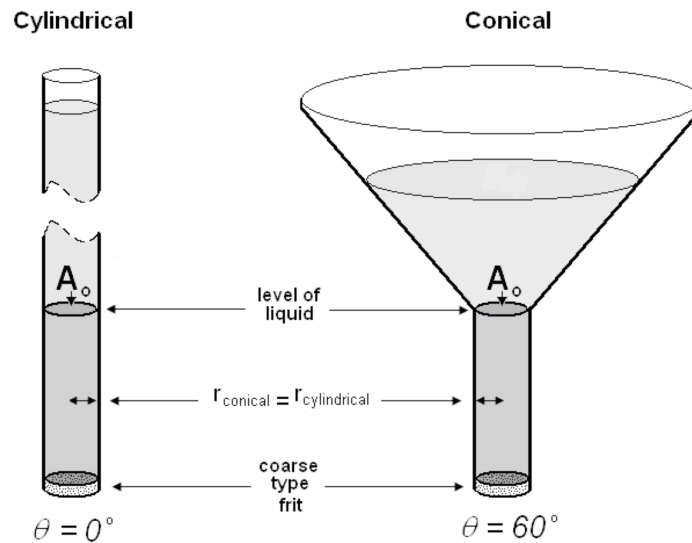


Figure 2 16: Cylindrical and conical foaming vessels.

Foam Volume Measurement

A TSPC-30S1-232 ToughSonic ® PC ultrasonic sensor was used to measure the distance to the surface of the foam (height). The corresponding foam volume was estimated from a calibration of volume vs. height. Three hundred height measurements were taken for each gas flowrate tested. Volume measurements had a precision of 0.05 cm³.

Surfactants

The surfactants used were two commercial flotation frothers F150 and MIBC (Table 1). Every concentration was replicated three times and the precision of concentration was 0.003%.

Temperature of the solution was measured prior to and after every test and was constant at 19.25 °C (± 0.05 °C).

Table 1 - Frothers used in foam volume experiments

Frother Type	Description	Molecular Weight (g/mol)	Chemical Formula
F150	Polypropylene glycol	425	H-(C ₃ H ₆ O) ₇ -OH
MIBC	Methyl isobutyl carbinol	102	CH ₃ CHCH ₃ CH(OH)CH ₃

Design of Experiment

Separate 3-factor, 2-level designs were performed to test the response of foamability, Σ , and the gas flowrate transition value, χ_o , to selected variables. Figure 3 shows the parameters tested for foamability: vessel type (cylindrical, conical); gas flowrate regime (flowrates below and above the transition value); and frother concentration (MIBC: 10/100 ppm, F150: 3/30 ppm). Separate analysis was preformed for the two frothers. Figure 4 shows the parameters tested for the gas transition value: vessel type (cylindrical, conical); frother concentration (low and high); and frother type (MIBC and F150). All studies were done at full factorial with three replicates of every condition (24 tests).

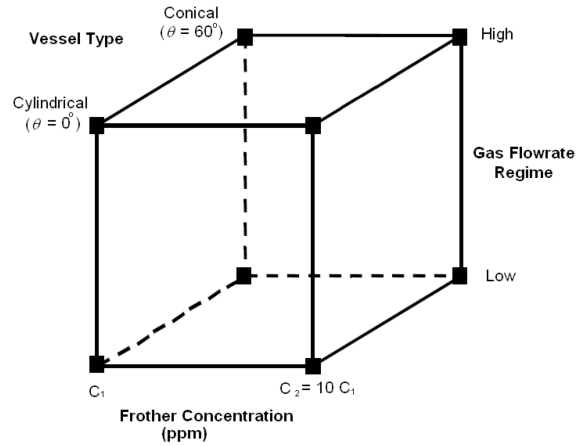


Figure 3: 3-factor, 2-level design used to test which parameters affect foamability.

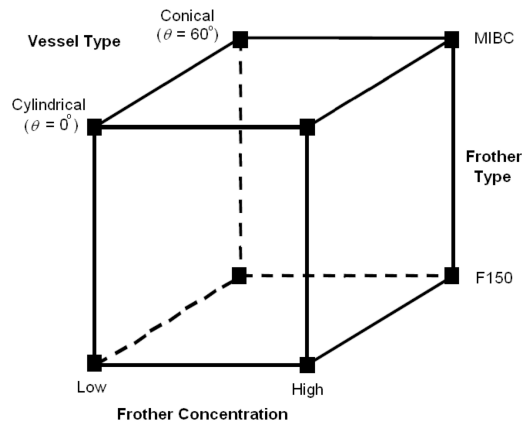


Figure 4: 3-factor, 2-level design used to test which parameters affect the gas transition value.

RESULTS

Foamability

Figures 5 to 8 show the foam volume results for the cylindrical and conical vessels at 3 ppm F150, 30 ppm F150, 10 ppm MIBC and 100 ppm MIBC, respectively. Foamability ranks upper cylindrical, lower conical, upper conical and lower cylindrical from greatest to least effect (where “upper” and “lower” refers to high and low gas flowrate, respectively). Table 2 lists the averaged foamability of upper conical and lower

cylindrical for both MIBC and F150 at all concentrations. The similarity of values may be an indication of similar processes at play, namely foam volume suppression.

Table 2 - Comparison of foamability for the upper gas flowrate regime of the conical vessel to the lower gas flowrate regime of the cylindrical vessel with different frothers and concentrations.

Σ	F150		MIBC	
	3 ppm	30 ppm	10 ppm	100 ppm
<i>Upper Conical</i>	1.405	2.834	0.435	4.473
<i>Lower Cylindrical</i>	1.469	3.065	1.085	2.841

Comparing the frothers, F150 is capable of creating more foam volume per ppm than MIBC. The foamabilities are comparable when one considers 30 ppm F150 and 100 ppm MIBC (Figure 6 and Figure 8, respectively). The foamability of 3 ppm F150 is marginally greater than 10 ppm MIBC. The difference in foamability of the conical and the cylindrical vessel is greater at the higher frother concentration (e.g., at 3 ppm F150 and 10 ppm MIBC, there is little difference in foam volume for the two vessels in the low flowrate regime).

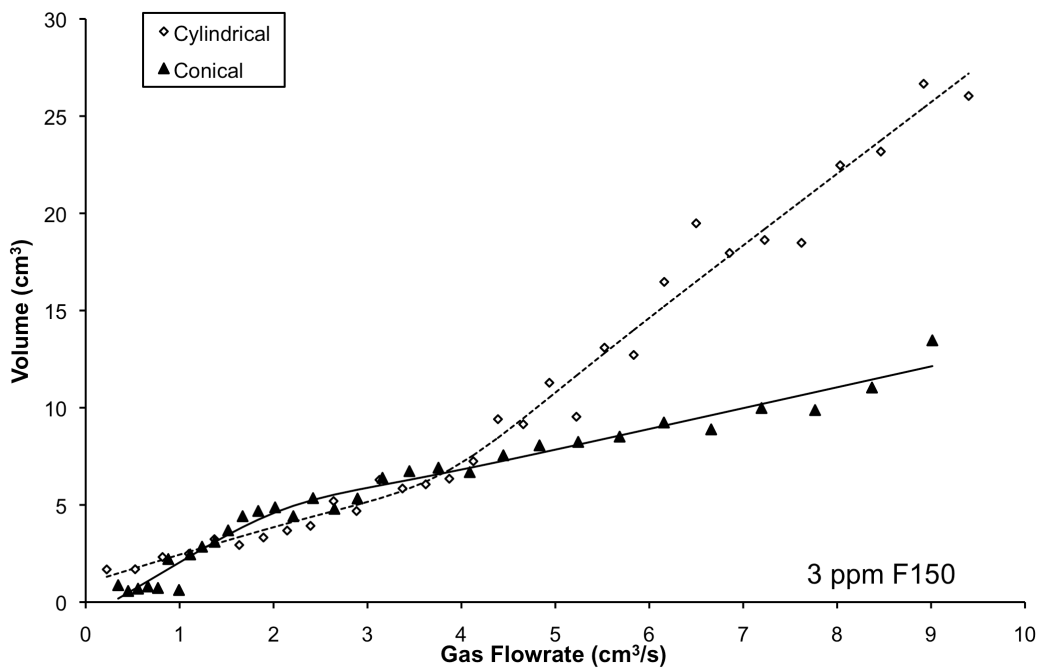


Figure 5: Foamability of 3 ppm F150

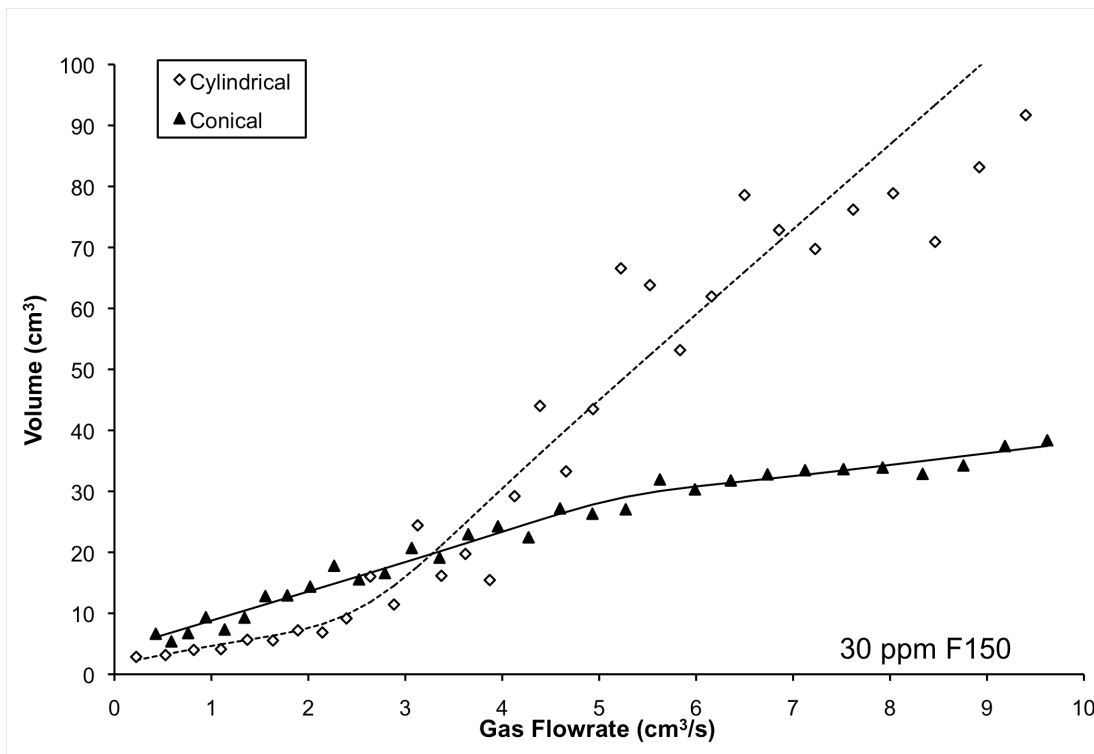


Figure 6: Foamability of 30 ppm F150

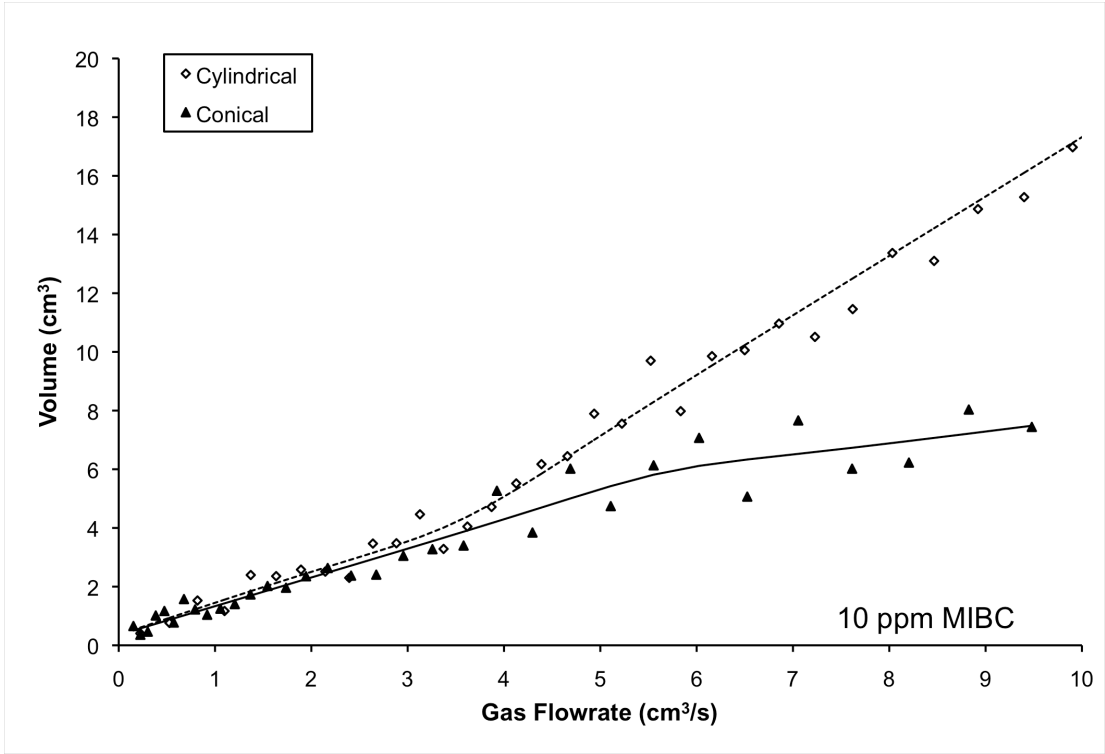


Figure 7: Foamability of 10 ppm MIBC

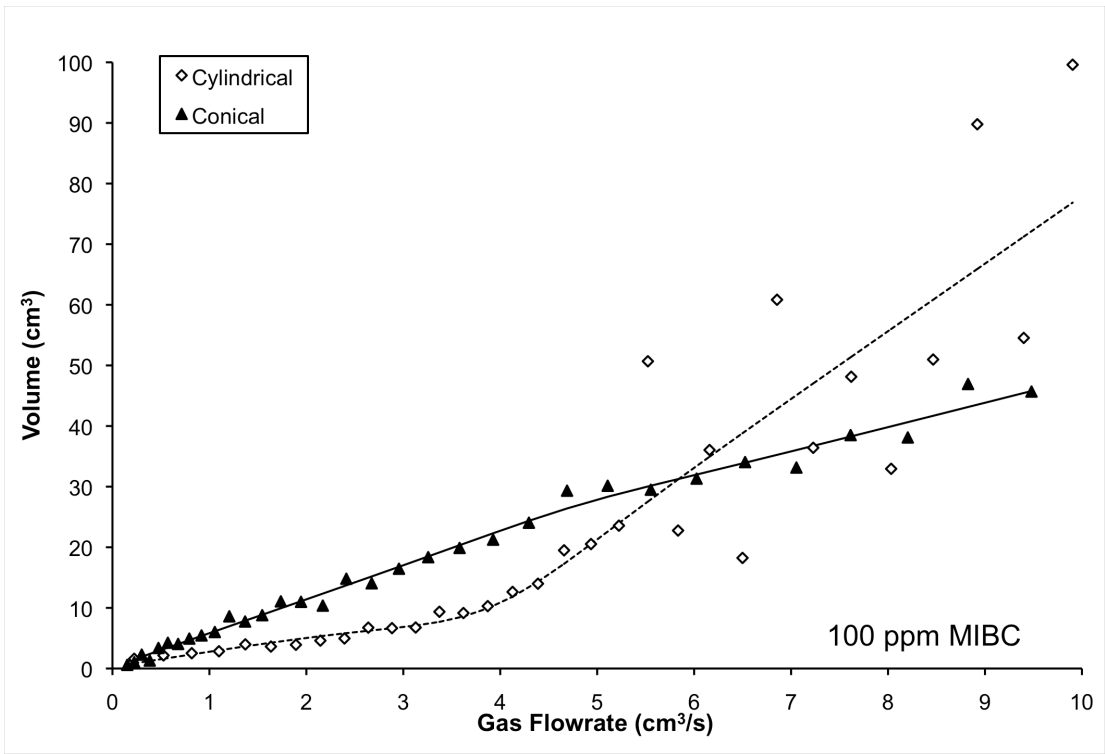


Figure 8: Foamability of 100 ppm MIBC

Transition Gas Flowrate Analysis

Regime change is evident in both the cylindrical vessel and the conical vessel. The origin is believed to be different in the two vessels. If that is so, then the gas flowrate that separates the regimes, i.e. the transition value, should be dependent on the vessel used. When the transition value was analyzed in respect to frother type and concentration, no relationship was evident. Nonetheless, frother type and concentration were included in a three-factor, two-level full factorial design along with vessel type in order to investigate any interactions in between the factors.

Table 3 lists all the factors, their resulting coefficient and their significance (P value > 0.05 is a significant interaction). The largest coefficient was the constant at 4.163 cm³/s (or in terms of J_g approximately 1.3 cm/s). Of the three factors, the only factor that was significant was the vessel. The significance of the vessel on the transition value supports the hypothesis that the regimes in the vessels are not related. Referring to Table 3, the transition values for the cylindrical and conical vessels are 3.53 cm³/s (1.08 cm/s) and 4.79 cm³/s (1.28 cm/s), respectively.

Table 3- Coefficients of interaction for transition gas flowrate values

Factor Name	Coefficient	P (2 Tail)
Constant	4.163	0.0000
Vessel	0.632	0.0159
Frother Type	0.055	0.8166
Concentration	-0.230	0.3406
Vessel x Frother Type	0.463	0.0657
Vessel x Concentration	0.096	0.6876
Frother Type x Concentration	-0.970	0.0008
Vessel x Frother Type x Concentration	-0.508	0.0457

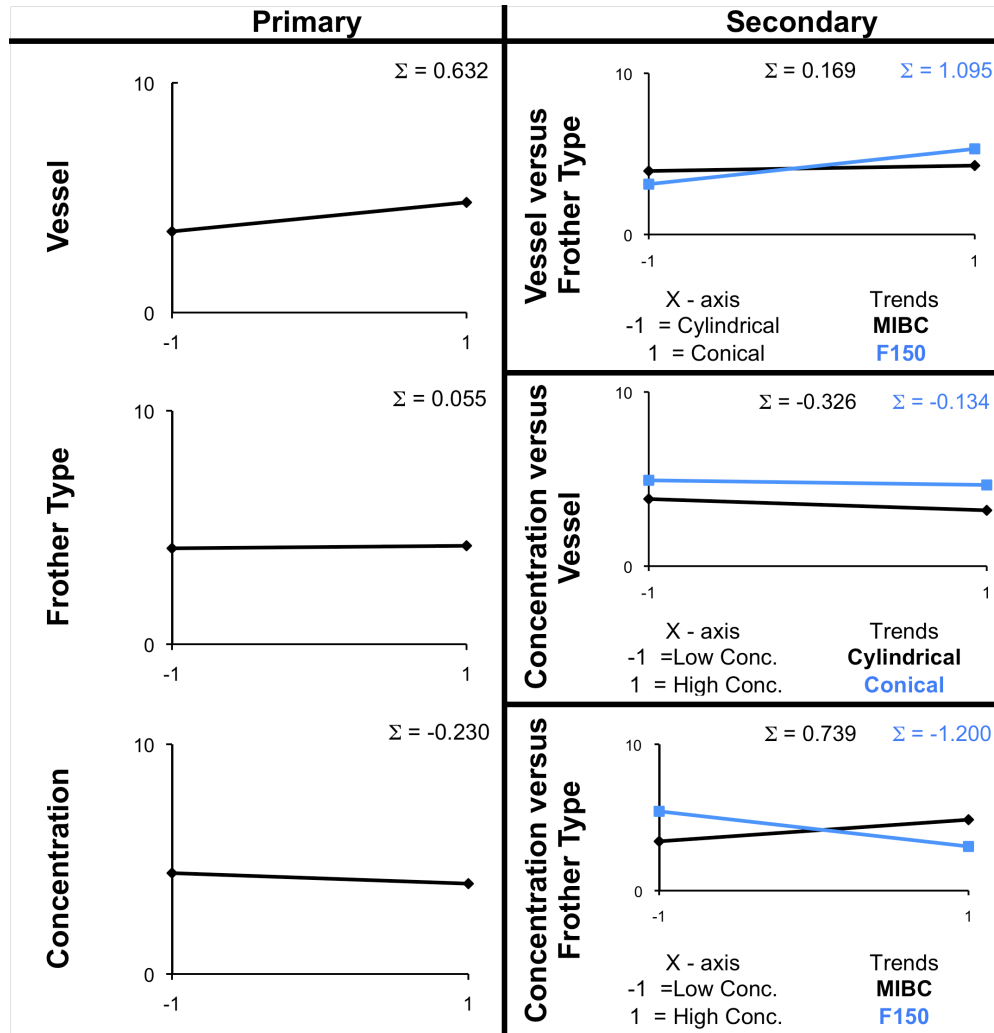


Figure 9: Transition gas flowrate value, primary and secondary interactions.

Although concentration was not a significant factor on its own, it was involved in significant interactions. Figure 9 shows both primary and secondary interactions. There is a weak secondary interaction between vessel and frother type, but it is not significant (Table 3). There is a strong and significant interaction between concentration and frother type. As concentration increases, the transition value increases for F150 and decreases for MIBC. This result is interesting as it is regardless of the vessel used. The finding may indicate that while the transition values between vessels are different and their

mechanisms may be distinct nevertheless there is a frother effect on both, i.e., the system chemistry affects the transition gas flowrate despite differences in mechanism.

Foamability

Separate analysis was done for F150 and MIBC. The response, foamability (Σ), was tested for sensitivity against the vessel used, the frother concentration and the gas flowrate regime. Tables 4 and 5 list the coefficients and their significance for F150 and MIBC, respectively. All primary, secondary and tertiary interactions are significant.

Table 4- Coefficients of interaction for F150

Factor Name	Coefficient	P (2 Tail)
Constant	3.973	0.0000
Vessel	-1.578	0.0000
Concentration	1.905	0.0000
Gas	1.143	0.0000
Vessel x Concentration	-1.069	0.0000
Vessel x Gas	-2.140	0.0000
Concentration x Gas	0.956	0.0000
Vessel x Concentration x Gas	-1.220	0.0000

Table 5- Coefficients of interaction for MIBC

Factor Name	Coefficient	P (2 Tail)
Constant	3.722	0.0000
Vessel	-1.098	0.0000
Concentration	2.597	0.0000
Gas	1.343	0.0000
Vessel x Concentration	-0.554	0.0046
Vessel x Gas	-1.513	0.0000
Concentration x Gas	1.125	0.0000
Vessel x Concentration x Gas	-1.149	0.0000

Figure 10 illustrates the primary interactions of the three factors for MIBC and F150. For both frothers, the response to each factor is similar. The strongest interaction is that for concentration. This is expected, as transient foams prepared with short-chained alcohols (i.e., frothers) are known to have a sensitivity to concentration (Pugh, 1996). The highest foamability is seen at high gas flowrates in the cylindrical vessel. This foamability

response strongly influenced the coefficient result for vessel and gas flowrate regime. As a whole, moving to high gas flowrate or to the cylindrical vessel results in greater foamability. The coefficients would be comparable to the concentration effect if the conical vessel did not have its higher stability region at low gas flowrates unlike the case for the cylindrical vessel.

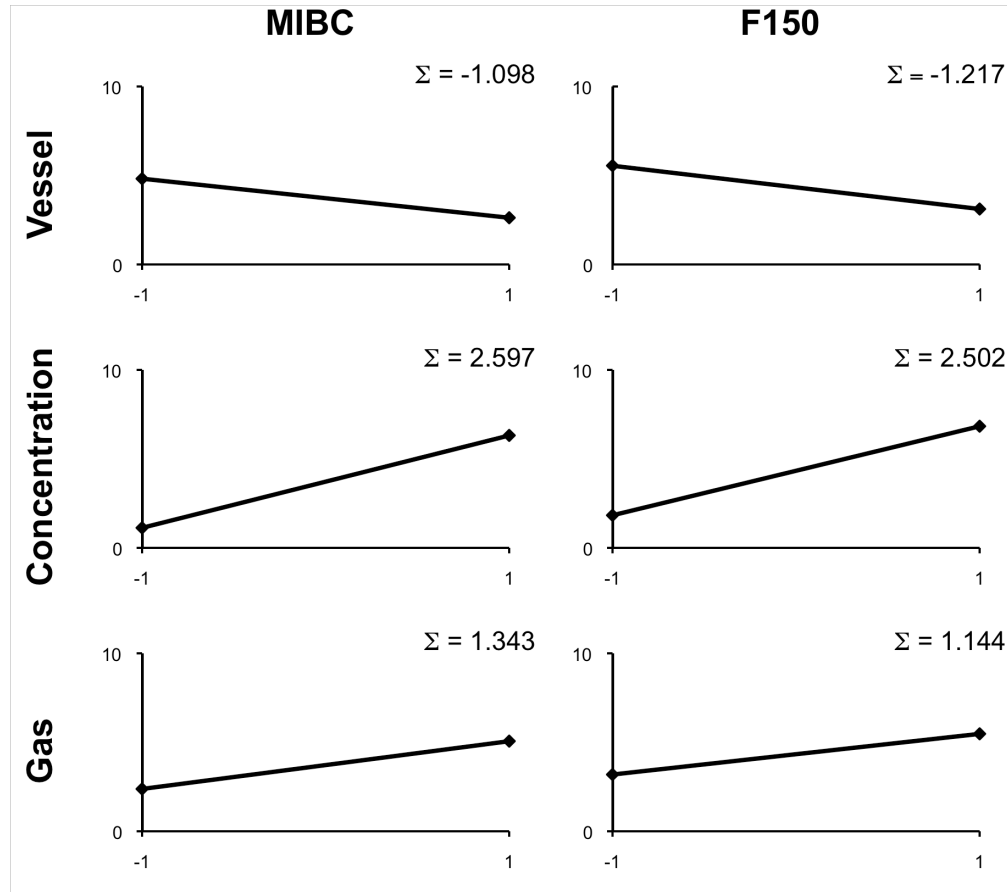


Figure 10: Primary interaction for foamability of MIBC and F150.

The secondary interactions are illustrated in Figure 11. MIBC and F150 show striking similarities in their interactions. There is little to no interaction for the vessel versus concentration as well for gas flowrate versus concentration. The largest interaction is gas flowrate versus vessel. The relevance of this interaction is that the gas flowrate and the vessel can have a large effect on the stability of the foam. This is especially true of the

cylindrical vessel where foamability can increase by approximately 3 Σ regardless of the frother concentration used. It would be for that reason that one should use a conical vessel for frother studies as opposed to a cylindrical vessel, because the conical vessel has less sensitivity to gas flowrate.

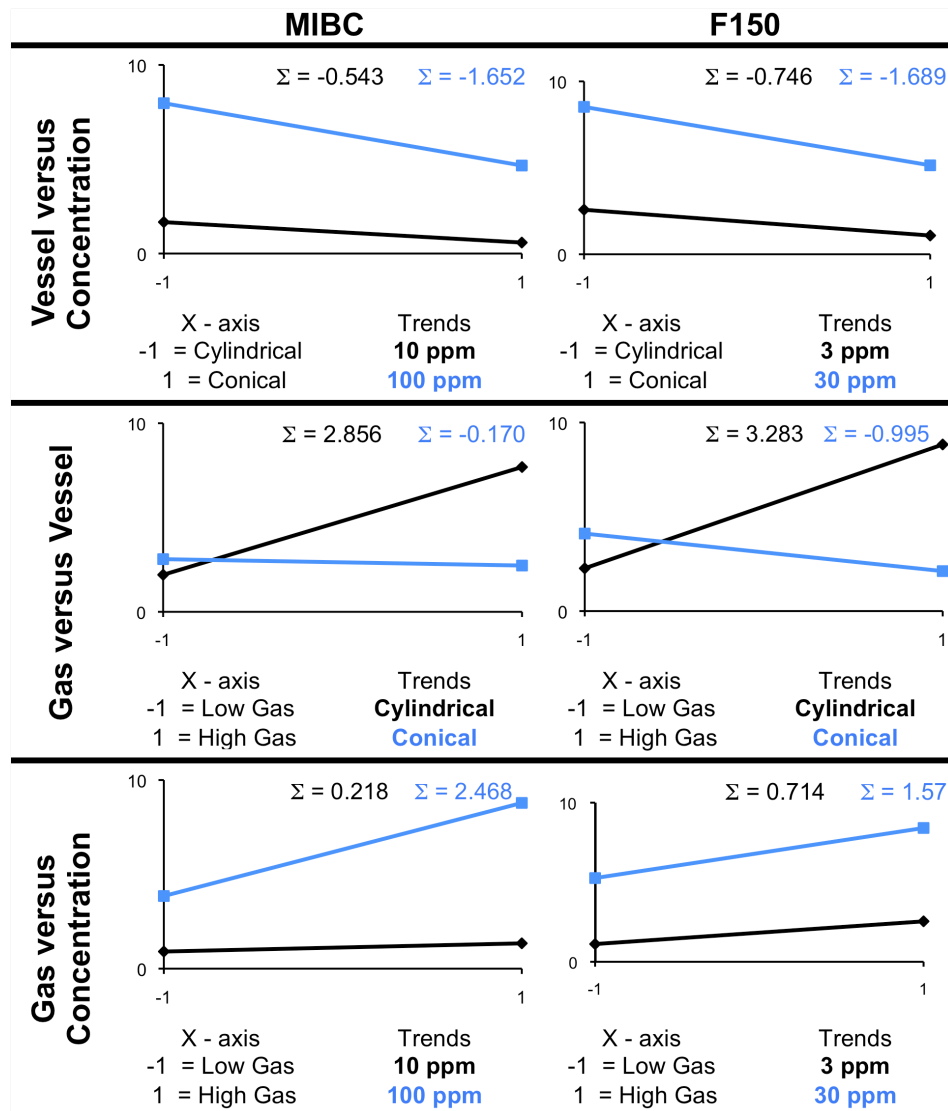


Figure 11: Secondary interaction for foamability of MIBC and F150.

Although similar, there are differences between the frothers. In the gas flowrate versus concentration interaction (Figure 11), MIBC increases stability considerably going from

10 ppm to 100 ppm, while F150 shows a more modest increase. The proposed stabilizing force for frothers is the Gibbs-Marangoni elasticity. Wang and Yoon (2008) measured the elasticity of MIBC and PPG400 (a similar molecule to F150, which alternatively is referred to as PPG425) and reported elasticities of 0 to 10 mN/m for MIBC (10 and 100 ppm, respectively) and 100 to 550 mN/m for PPG400 (3 and 30 ppm respectively). If this is true for our system as well, then the stability mechanism would be active for MIBC only at the higher concentration (100 ppm).

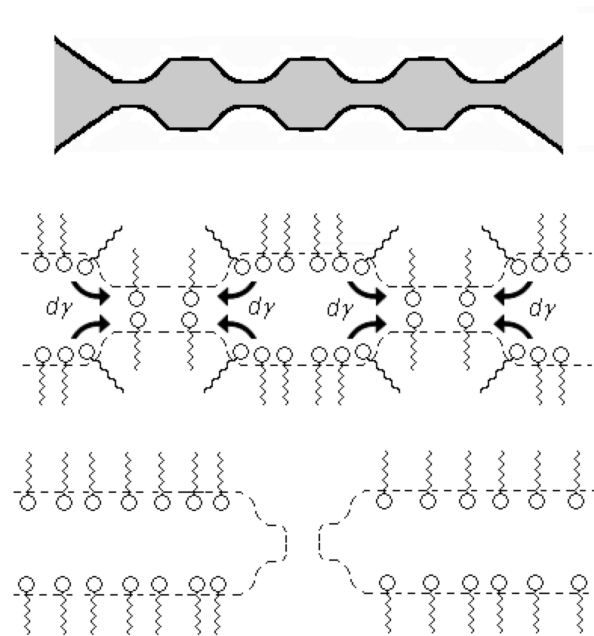


Figure 12: A strong Gibbs-Marangoni effect may initiate film rupture by creating local tension, as illustrated.

Considering the gas flowrate versus vessel interaction (Figure 11), foamability decreases more for F150 than MIBC in the conical vessel as gas flowrate was increased. The proposed destabilizing mechanism for high gas flowrates in the conical vessel is kinematic forces in the bubbly zone. The turbulence of the bubbly zone conducts mechanical energy to the foam zone. F150, with its greater elasticity, may be destabilized

more by this turbulence than MIBC. Figure 12 shows a film undergoing perturbation (oscillations). In the same way that thin film thickness is restored due to the Gibbs-Marangoni effect, film rupture can be initiated when two perturbations are in close proximity. The forces locally put the film under tension which can cause rupture.

CONCLUSION

The vessel geometry used in foam stability measurements can have a strong effect on the measurements. The effect of gas flowrate is also an important variable; together these two factors must be considered when examining foaming properties of surfactants, especially with weak surfactants like commercial frothers.

A transition from one foam stability regime to another occurs at a certain gas flowrate in both conical and cylindrical vessels. The regimes and transition gas flowrate reflect different mechanisms in the two vessels. For the cylindrical vessel, the transition occurs when conditions change from foam suppression to foam growth. This effect complicates examination of frother foaming properties. For the conical vessel the regime change was associated with a transition from a quiescent to turbulent bubbly zone. Foaming properties of a frother are best determined with a variable area vessel at low gas flowrate.

REFERENCES

- ATA, S., AHMED, N. & JAMESON, G. J. 2003. A study of bubble coalescence in flotation froth. *International Journal of Mineral Processing*, 72, 255-266.
- PUGH, R. 1996. Foaming, foam films, antifoaming and defoaming. *Advances in Colloid and Interface Science*, 64, 67-142.

WANG, L. & YOON, R. 2008. Effects of surface forces and film elasticity on foam stability. *International Journal of Mineral Processing*, 85, 101-110.